**Differential modulation of ventral tegmental area circuits by the nociceptin/orphanin FQ system**

Joseph R. Driscoll[1,2]; Tanya L. Wallace[1]; Kasra A. Mansourian[2]; William J. Martin[1]; Elyssa B. Margolis[2]

[1]BlackThorn Therapeutics
780 Brannan Street
San Francisco, CA 94103

[2]UCSF Weill Institute of Neurosciences
Department of Neurology
University of California, San Francisco
675 Nelson Rising Lane
Box 0444
San Francisco, CA 94143, USA

JRD, TLW, WJM and EBM designed the studies; JRD, KAM, and EBM collected the data; JRD, KAM, and EBM analyzed the data; JRD, TLW, WJM and EBM wrote the manuscript.

Corresponding Author:
Elyssa B. Margolis
elyssa.margolis@ucsf.edu
University of California, San Francisco
675 Nelson Rising Lane
Box 0444
San Francisco, CA 94143, USA
Phone: (415) 353-4793

**Acknowledgements**
We would like to thank Benjamin J. Snyder and Venkateswaran Ganesh for their technical assistance. We also thank Howard L. Fields for helpful comments on the manuscript.

**Conflict of interest**
Yes, TLW and WJM are employees of and shareholders in BlackThorn Therapeutics, which is evaluating BTRX-246040 for the treatment of neurobehavioral disorders.

**Funding**
This work was supported through a sponsored research agreement from BlackThorn Therapeutics, Inc. to the University of California, San Francisco, and by National Institutes of Health grant number R01 DA042025 to E.B.M.

**Abstract**

The neuropeptide nociceptin/orphanin FQ (N/OFQ) can be released by stressors and is associated with disorders of emotion regulation and reward processing. N/OFQ and its receptor, NOP, are enriched in dopaminergic pathways, and intra-ventricular agonist delivery decreases dopamine levels in the dorsal striatum, nucleus accumbens (NAc), and ventral tegmental area (VTA). We used whole cell electrophysiology in acute rat midbrain slices to investigate synaptic actions of N/OFQ. N/OFQ was primarily inhibitory, causing outward currents in both immunocytochemically identified dopaminergic (tyrosine hydroxylase positive (TH(+)) and non-dopaminergic (TH(-)) VTA neurons (effect at 1 $\mu$M: 20 $\pm$ 4 pA). Surprisingly, this effect was mediated by augmentation of postsynaptic $GABA_AR$ currents, unlike the substantia nigra pars compacta (SNc), where the N/OFQ induced outward currents were $K^+$ channel dependent. A smaller population, 19% of all VTA neurons, responded to low concentrations N/OFQ with inward currents (10 nM: -11 $\pm$ 2 pA). Following 100 nM N/OFQ, the response to a second N/OFQ application was markedly diminished in VTA neurons (14 $\pm$ 10% of first response), but not in SNc neurons (90 $\pm$ 20% of first response). N/OFQ generated outward currents in medial prefrontal cortex (mPFC)-projecting VTA neurons, but inward currents in a subset of posterior anterior cingulate cortex-projecting VTA neurons. While N/OFQ inhibited NAc-projecting VTA cell bodies, it had little effect on electrically or optogenetically evoked terminal dopamine release in the NAc measured *ex vivo* with fast scan cyclic voltammetry. These results extend our understanding of the N/OFQ system in brainstem circuits implicated in many neurobehavioral disorders.

**Significance statement**

The neuropeptide nociceptin/orphanin FQ (N/OFQ) and its receptor (NOP) are engaged under conditions of stress and are associated with reward processing disorders. Both peptide and receptor are highly enriched in ventral tegmental area (VTA) pathways underlying motivation and reward. Using whole cell electrophysiology in rat midbrain slices we found: 1) NOPs are functional on both dopaminergic and non-dopaminergic VTA neurons; 2) N/OFQ differentially regulates VTA neurons based on neuroanatomical projection target; and 3) repeated application of N/OFQ produces evidence of receptor desensitization in the VTA but not the SNc. These results reveal candidate mechanisms by which the NOP system regulates motivation and emotion.

**Introduction**

Nociceptin/Orphanin FQ (N/OFQ) and its receptor (NOP) make up a neuropeptide signaling system de-orphaned in 1995 (Meunier et al., 1995; Reinscheid et al., 1995) that is engaged under conditions of stress (Ciccocioppo et al., 2000; Devine et al., 2001; Fernandez et al., 2004; Green et al., 2007; Green and Devine, 2009; Leggett et al., 2007, 2006; Nativio et al., 2012; Nicholson et al., 2002). The NOP is a G-protein coupled 7-transmembrane domain receptor that canonically signals through Gi/o proteins, post-synaptically activating G-protein coupled inward-rectifying potassium channels (GIRKs), or pre-synaptically reducing probability of neurotransmitter release via inhibition of N-type calcium channels (Hawes et al., 2000; Knoflach et al., 1996; New and Wong, 2002; Vaughan and Christie, 1996). While amino acid sequence homology has led some to categorize the NOP as an opioid receptor (Bunzow et al.,

1994; Meunier et al., 1995; Mollereau et al., 1994; Wang et al., 1994), NOP activation is not blocked by naloxone, a non-selective opioid receptor antagonist that was originally used to classify responses as opioid receptor mediated, blocking activation at mu, delta, and kappa opioid receptors (MOPs, DOPs, and KOPs, respectively) (Gintzler et al., 1997; Mogil and Pasternak, 2001; Reinscheid et al., 1996, 1995). Furthermore, the known endogenous opioid peptides (dynorphins, enkephalins, and endorphins) do not bind to the NOP, and N/OFQ does not bind to the MOP, DOP, or KOP (Ma et al., 1997; Meng et al., 1996; Sim et al., 1996). Because of the extensive amino acid sequence homology and these distinct pharmacological properties, N/OFQ and the NOP are most appropriately subclassified as non-classical members of the opioid family (Cox et al., 2015; Toll et al., 2016).

N/OFQ and the NOP are highly enriched in the ventral tegmental area (VTA), dorsal striatum, nucleus accumbens (NAc), medial prefrontal cortex (mPFC), and central nucleus of the amygdala (Berthele et al., 2003; Neal et al., 1999; Parker et al., 2019). The VTA is the major source of dopamine to limbic forebrain regions and plays a key role in brain networks that coordinate motivation and learned appetitive behaviors (Fields et al., 2007). Activity of VTA dopamine neurons is associated with salience and reward prediction, while destruction of these neurons results in motivational deficits (Fields et al., 2007; Kim et al., 2012; Mohebi et al., 2019; Morales and Margolis, 2017; Tsai et al., 2009; Ungerstedt, 1971; Wise, 2005; Witten et al., 2011). Intracerebroventricular (ICV) injections of N/OFQ produce a decrease in extracellular dopamine in the dorsal striatum and NAc, and some midbrain putative dopamine cell bodies are inhibited by NOP activation (Di Giannuario and Pieretti, 2000; Lutfy et al., 2001; Murphy et al., 1996; Murphy and Maidment, 1999; Vazquez-DeRose et al., 2013; Zheng et al., 2002).

Dysregulation of the N/OFQ system has been associated with disorders of motivated responding (Civelli, 2008), and the N/OFQ system has been investigated as a novel therapeutic target for major depressive disorder and alcohol use disorder (Witkin et al., 2019), however understanding the involvement of the N/OFQ system in these behaviors remains a challenge. In fact, in some cases, activation and blockade of NOPs paradoxically produce the same behavioral outcomes, such as with alcohol consumption (Ciccocioppo et al., 2014, p. 7716; Kuzmin et al., 2007; Rorick-Kehn et al., 2016) and anxiety-related behaviors (Dautzenberg et al., 2001; Fernandez et al., 2004; Gavioli et al., 2002; Green et al., 2007; Jenck et al., 1997; Kamei et al., 2004; Varty et al., 2008; Vitale et al., 2006). Such observations may be explained by off-target effects of N/OFQ, activation of N/OFQ sensitive neural circuits that compete for behavioral control, or receptor desensitization.

Here we investigated the basic physiology of N/OFQ responses in VTA neurons to better characterize how N/OFQ contributes to motivation and reward processing. To confirm that our physiological responses to N/OFQ were due to NOP activation we utilized the selective NOP antagonist BTRX-246040 (Toledo et al., 2014) to block N/OFQ responses. We observed similar N/OFQ effects on both dopamine and non-dopamine VTA neurons. Importantly, we found that responses to N/OFQ differ between VTA and substantia nigra pars compacta (SNc) in mechanism of inhibition and functional desensitization measures. Furthermore, we found that for VTA neurons, N/OFQ responses vary by the projection target. For example, N/OFQ induced small inward currents preferentially in VTA neurons that project to the posterior anterior cingulate cortex (pACC). In addition, although NAc-projecting cell bodies were inhibited by NOP activation, N/OFQ did not inhibit dopamine release at terminals in the NAc. Together these

observations indicate that NOP actions vary not only by brain region and neuron subpopulation, but also by structural localization within a neuron.

## Materials and Methods

*Electrophysiology*: Most experiments were completed in tissue from male Sprague Dawley rats, p22 – p36, except mechanism experiments which were completed in tissue from adult rats (>200g). Rats were anesthetized with isoflurane, and brains were removed. The brains were submerged in Ringer's solution containing (in mM): 119 NaCl, 2.5 KCl, 1.3 $MgSO_4$, 1.0 $NaH_2PO_4$, 2.5 $CaCl_2$, 26.2 $NaHCO_3$, and 11 glucose saturated with 95% $O_2$–5% $CO_2$ and horizontal brain slices (150 μm thick) containing the VTA were prepared using a Vibratome (Leica Instruments, Nussloch, Germany). Slices were and allowed to recover at 35°C for at least 1 hr before recordings were initiated. The same Ringer's solution was used for cutting, recovery, and recording.

Individual slices were visualized under an Olympus BX50WI microscope (Olympus Life Science Solutions, Waltham, MA) with differential interference contrast optics and near infrared illumination, using an Andor xIon+ camera, and Andor Solis imaging software (Andor Technology Ltd, Belfast, Northern Ireland), or under a Zeiss Axio Examiner.D1 with differential interference contrast optics, near infrared illumination, and Dodt contrast, using a monochrome Axiocam 506 (Zeiss International, Oberkochen, Germany). Whole-cell patch-clamp recordings were made at 33°C using 2.5– 4M pipettes containing (in mM): 123 K-gluconate, 10 HEPES, 0.2 EGTA, 8 NaCl, 2 MgATP, and 0.3 $Na_3GTP$, pH 7.2, osmolarity adjusted to 275 mOsm. Biocytin (0.1%) was added to the internal solution for post hoc identification.

Recordings were made using an Axopatch 1-D (Axon Instruments, Union City, CA), filtered at 2 kHz, and collected at 20 kHz using IGOR Pro (Wavemetrics, Lake Oswego, OR) or an IPA amplifier with SutterPatch software (Sutter Instrument, Novato, CA) filtered at 1 kHz and collected at 10 kHz. Liquid junction potentials were not corrected during recordings. Hyperpolarization-activated cation currents ($I_h$) were recorded by voltage clamping cells and stepping from -60 to -40, -50, -70, -80, -90, -100, -110, and - 120 mV. The $I_h$ magnitude was measured as the difference between the initial response to the voltage step after the capacitive peak and the final current response.

Pharmacology experiments were completed in voltage-clamp mode (V = -60 mV) to measure changes in membrane current. Series resistance was monitored online by measuring the peak of the capacitance transient in response to a −4 mV voltage step applied at the onset of each sweep. Input resistance was measured using the steady state response to the same voltage step. Upon breaking into the cell, at least 10 min was allowed for the cell to stabilize and for the pipette internal solution to dialyze into the cell. Drugs were applied via bath perfusion at a flow rate of 2 mL/min or pressure ejection using a SmartSquirt micro-perfusion system (AutoMate Scientific, Berkeley, CA) coupled to a 250 μm inner diameter tubing outlet positioned nearby the recorded cell (within ~200 μm). N/OFQ (1 nM to 10 μM) was bath applied (5-7 min) or pressure injected (2 min) only after a 5 min stable baseline was achieved. Responses were similar to the two forms of N/OFQ application at the same concentrations. For instance at 100 nM, bath application 10.1 ± 1.5 pA, n = 21; pressure ejection 9.8 ± 2.1 pA, n = 12. Any cell that showed drift or did not maintain a consistent baseline current for the full 5 min period was removed from the analysis. All experiments where repeated N/OFQ applications are reported,

133 such as the desensitization experiments, were completed with bath application. To test that
134 observed N/OFQ-mediated effects were specific to NOP, the selective NOP antagonist BTRX-
135 246040 (10 or 100 nM) was applied for 10 min prior to N/OFQ. As there was no statistical
136 difference in the mean amplitude of response for bath application and pressure injection the
137 results were combined for the analysis.
138 For iontophoresis experiments, the holding current was set to -50 mV to increase the
139 driving potential for $Cl^-$. GABA (100 mM, pH adjusted to 4.9 with 37% HCl) was prepared daily
140 and the GABA-containing pipette was positioned approximately 50 µm away from the recorded
141 neuron. Negative retention current (approximately -35 nA) was applied to the GABA pipette,
142 interrupted by positive ejection current pulses (100 ms) once every 30 s, with the intensity
143 adjusted so that the response amplitude was in the range of 100-300 pA.
144 Stock solutions of drugs were made in advance, stored at -20°C, and diluted into aCSF
145 immediately before application. N/OFQ was obtained from Tocris (Minneapolis, MN) and diluted
146 to a 100 $\mu$M stock solution in $ddH_2O$. Stock BTRX-246040 was obtained from BlackThorn
147 Therapeutics and dissolved in DMSO (10 mM).
148 *Retrograde Tracer Injections*: Male Sprague Dawley rats, 21–100 d old, were
149 anesthetized with isoflurane. A glass pipette (30- to 50-µm tip) connected to a Nanoject
150 II/Nanoliter 2000 microinjector (Drummond Scientific Co.) was stereotaxically placed in the
151 mPFC (from bregma [in mm]: anteroposterior [AP], +2.6; mediolateral [ML], ±0.8; ventral [DV],
152 −4.0 from skull surface), the pACC (AP, 1.6; ML, ± 0.6; V, −3.5), or the NAc (AP, +1.5; ML, ±
153 0.8; V, −6.7). Neuro-DiI (7% in ethanol; Biotium) was slowly injected, 50.6 nL per side. Animals
154 were allowed to recover for 5 to 7 days while the retrograde tracer transported back to the cell
155 bodies. On the day of recording, the experimenter was blind to the location of retrograde tracer
156 injection (mPFC, pACC, or NAc) and slices were prepared as above. Projection neurons were
157 chosen by selecting cells observed as labeled using epiflorescent illumination. All injection sites
158 were histologically confirmed by a third party blind to the electrophysiology results to avoid bias.
159 N/OFQ responses were analyzed prior to unblinding. Animals with improper injection
160 placements or significant diffusion outside of the target region were rejected.
161 *Immunohistochemistry*: Slices were pre-blocked for 2 h at room temperature in PBS with
162 0.2% BSA and 5% normal goat serum, then incubated at 4°C with a rabbit anti-TH polyclonal
163 antibody (1:100; EMD Millipore, RRID: AB_390204). Slices were then washed thoroughly in
164 PBS with 0.2% BSA before being agitated overnight at 4°C with Cy5 anti-rabbit secondary
165 antibody (1:100; Jackson ImmunoResearch Labs Inc., West Grove, PA, RRID: AB_2534032)
166 and FITC streptavidin (6.5 µL/mL). Sections were rinsed and mounted on slides using Bio-Rad
167 Fluoroguard Antifade Reagent mounting media and visualized with an Axioskop FS2 Plus
168 microscope with an Axiocam MRm running Neurolucida (MBF Biosciences, Williston, VT).
169 Neurons were only considered TH(−) if there was no colocalization of biocytin with TH signal
170 and the biocytin soma was in the same focal plane as other TH(+) cell bodies. Primary
171 antibodies were obtained from Millipore Bioscience Research Reagents or Millipore, secondary
172 antibodies were obtained from Jackson ImmunoResearch Laboratories, and all other reagents
173 were obtained from Sigma Chemical.
174 *Fast Scan Cyclic Voltammetry*: Male Sprague Dawley rats, 21–26 d old, or *Th::Cre*
175 transgenic rats (Witten et al., 2011), 46-51 d old at the time of virus injection, were used in these
176 studies. Th::Cre rats were injected with the Cre dependent ChR2 expressing virus (AAV2-Ef1a-

177 DIO-hChR2(H134R)-mCherry, titer 5.1X10$^{12}$ viral particles/mL, UPenn viral core) bilaterally into
178 the VTA 500 nL per side (AP, −5.3; ML, ± 0.4; DV, −8.2 mm from bregma). Five weeks later,
179 coronal slices (400 μm) containing the NAc were prepared for voltammetry measurements. The
180 use of Cre dependent ChR2 expression allowed selective optical control of VTA dopamine
181 terminals in the NAc.
182 Extracellular dopamine release was achieved using either electrical (in wild-type
183 Sprague Dawley rats) or 470 nm light (in Th::Cre rats) stimulation. Stimulation parameters were
184 the same for both electrical and optical stimulation (10 Hz, 2 pulses, 4 ms). Electrochemical
185 recordings were made using carbon fiber electrodes fabricated from T-650 carbon fiber (7 μm
186 diameter, gift from Dr. Leslie Sombers (NCSU)) that was aspirated into a borosilicate glass
187 capillary (0.6 × 0.4 mm or 1.0 × 0.5 mm diameter, King Precision Glass Inc., Claremont, CA)
188 and pulled using a PE-22 puller (Narishige, Tokyo, Japan). Carbon fiber electrodes were
189 positioned 80 μm into the tissue either between the bipolar tips of the stimulating electrode or
190 directly in front of an optical fiber connected to an LED emitting 470 nm light (7-10 mW). The
191 potential of the carbon fiber electrode was held at -0.4 V relative to the Ag/AgCl reference
192 electrode. A triangle wave form was passed through the carbon fiber driving the potential from -
193 0.4 V to +1.3 V and back to -0.4 V at a rate of 400 V/s, at 60 Hz for conditioning and 10 Hz for
194 data collection. Data were collected with a WaveNeuro fast scan cyclic voltammetry (FSCV)
195 potentiostat (Pine Research, Durham, NC) using HDCV acquisition software package (freely
196 available through UNC Department of Chemistry). HDCV Acquisition Software was used to
197 output the electrochemical waveform and for signal processing (background subtraction, signal
198 averaging, and digital filtering (4-pole Bessel filter, 2.5 kHz)). Dopamine release was stimulated
199 at 2 min intervals for electrical stimulation and 3 min intervals for optical stimulation. The
200 difference in stimulation invervals was to decrease rundown of the dopamine release signal that
201 can be particularly strong in optical experiments as reported in (Bass et al., 2013; O'Neill et al.,
202 2017). Mean background currents from 1 sec of data prior to stimulation were removed by
203 subtraction of cyclic voltammograms for each trial.
204 *Data Analysis*: For electrophysiology, effects of N/OFQ were statistically evaluated in
205 each neuron by binning data into 30 s data points and comparing the last eight binned pre-drug
206 points to the last eight binned points during drug application using Student's unpaired *t* test. To
207 evaluate the output of this analysis approach, we performed a subsequent sliding window
208 analysis on this classified data from TH(+) neurons that were tested with 10 nM N/OFQ (Figure
209 1-1). The results of this analysis are consistent with this classification scheme identifying drug
210 responses and a lack of contamination by drift in individual recordings. For within cell
211 comparisons of N/OFQ responses, responses were compared with a Student's paired *t* test. $P$
212 $< 0.05$ was required for significance in all analyses. Differences between neuron populations
213 were tested using two-tailed permutation analyses unless otherwise indicated. Violin plots were
214 constructed by calculating the kernal density estimate, made using a Scott estimator for the
215 kernal bandwidth estimation. The kernel size was determined by multiplying the Scott bandwidth
216 factor by the standard deviation of the data within each bin. Each individual violin plot was
217 normalized to have an equal area under the curve. Time course figures are averages of the
218 binned current traces for all cells time locked to the start of drug application. $EC_{50}$ was estimated
219 by fitting the concentration response data with the Hill equation. Results are presented as mean

220 and standard error of the mean (SEM). Custom code created for analyses here are publicly
221 available at https://osf.io/c8gu7/?view_only=63ea4c0623b54e46a4efaccc450a89c6.

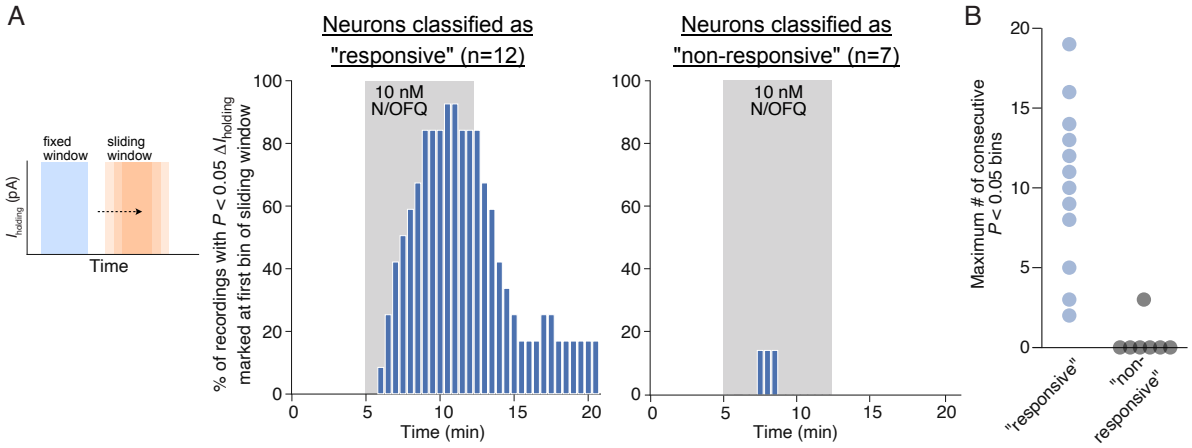


**Extended Data:** To evaluate our within cell statistical comparisons to identify "responsive" vs "non-responsive" neurons, in particular to test the possibility that drift might contribute to some of our identified drug effects, we conducted a sliding window analysis on a subset of our drug responses (all TH positive neurons tested with bath application of 10 nM N/OFQ). Further, any increase in statistically significant sliding windows during drug washout compared to the static baseline would suggest underlying $I_{holding}$ drift. We compared all 4 minute windows from pre-drug application through drug washout to a fixed "baseline" window (the 4 min preceding the onset of the drug). To create the windows, $I_{holding}$ of each recording was binned into 30 second intervals and assigned a bin number (1, 2, 3 Ö n). The "baseline" 8 bin (4 min) window was compared with the target 4 min window by way of a student's unpaired t-test. The *P* value and significance of the comparison was then corrected using the Bonferroni method for multiple comparisons. The alignment of the sliding window was then increased by a single bin and the comparison repeated, resulting in an array that represents all significant 4 minute intervals for each drug effect. The resulting arrays were plotted as a histogram representing, at the initial bin time of the sliding window, the proportion of recordings in which this calculation was significantly different from the fixed baseline target window (A). In the neurons previously classified as "responsive" by a single "baseline" compared to "drug" window comparison, the rising left edge of the histogram begins to plateau around the 4$^{th}$ minute of drug application, consistent with the plateau of the mean effects across all cells reported in Figure 1D. Further, consistent with washout reversal of N/OFQ effects in most but not all neurons, the proportion of significant bins falls off as soon as N/OFQ application was terminated. That both the rise and fall of the frequencies of significant windows are time locked to the drug application suggests the response classification scheme is reliable. In neurons previously classified as "non-responsive" only one neuron had any significant windows, with 3 sliding window locations where this analysis yielded $P < 0.05$, suggesting that there was not systematic drift in these "non-responsive" neurons. In addition, a scatter plot (B) indicates the maximum number of consecutive significant sliding windows for each cell analyzed, because a well-behaved change in $I_{holding}$ in response to the drug application should be detected in consecutive sliding windows. This graph shows that 8/12 neurons that were classified as "responsive" have more consecutive sliding windows different from baseline than the maximum found in "non-responsive" neurons. This analysis was conducted using a custom script created in Python (available at https://osf.io/c8gu7/?view_only=63ea4c0623b54e46a4efaccc450a89c6).

222

223 **Results**

224 *N/OFQ effects on holding current in VTA dopamine and non-dopamine neurons*

225 To test the postsynaptic responses of VTA neurons to N/OFQ, we made *ex vivo* whole
226 cell voltage clamp recordings ($V_m$ = -60 mV). N/OFQ application changed the holding current in
227 70% (60/86) of neurons tested in the VTA (10 nM; 86 neurons from 59 rats; Fig. 1A,B). The
228 majority of responses were relatively small outward currents (73% of responsive neurons,

229 44/60; 51% of all neurons tested, 44/86; mean response magnitude = 15 ± 2 pA; Fig. 1D). In
230 many cases the holding current returned to baseline during N/OFQ washout, as in Fig. 1A,
231 however in some cases we observed only partial recovery. Using post-hoc
232 immunocytochemistry, we analyzed TH content in each histologically recovered neuron and
233 found that N/OFQ inhibited both confirmed dopamine and non-dopamine neurons in similar
234 proportions (of 44 inhibited neurons from 38 rats, 26 neurons from 23 rats were identified:
235 TH(+): 12/26; TH(-): 14/26). The magnitudes of responses were also similar between confirmed
236 dopamine and non-dopamine neurons (TH(+): 12 ± 2 pA (n = 12); TH(-): 9 ± 2 pA (n = 14); $p$ =
237 0.3 two tailed permutation test; Fig. 1C). The $EC_{50}$ for these outward currents is in the nM range
238 (8 ± 6 nM; Fig. 1E).

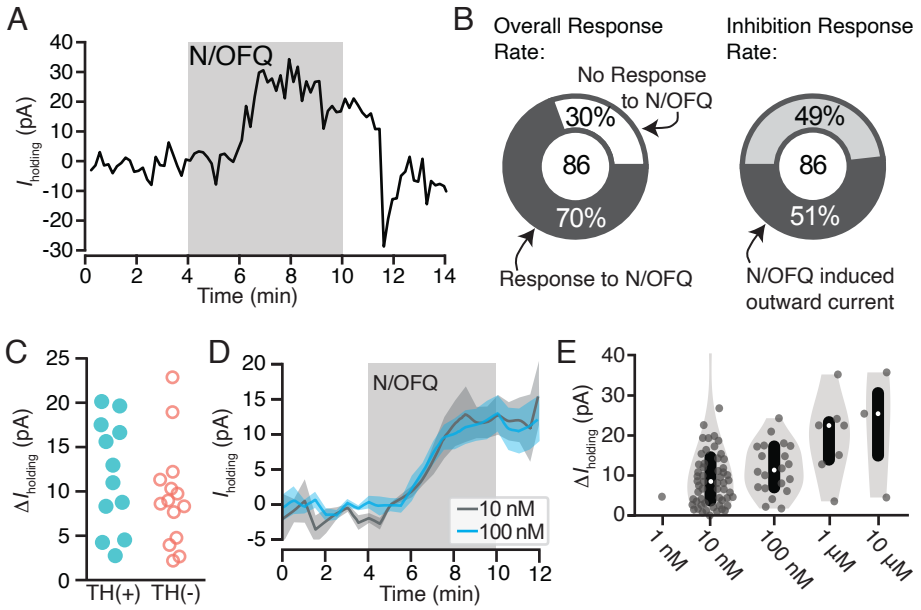


**Figure 1: N/OFQ induced outward currents in a subset of VTA neurons.** A: Example voltage clamp recording ($V_{clamp}$ = -60 mV) of a VTA neuron that responded to N/OFQ with an outward current. B: Across recordings in neurons from control rats, the majority of VTA neurons responded to 10 nM N/OFQ application (60 out of 86 neurons responded). Forty four out of 60 responses were outward currents. C: A subset of recorded neurons were recovered following whole cell recording and immunocytochemically identified for TH content, a marker for dopamine neurons. Outward currents of similar magnitudes were observed in TH(+) and TH(-) neurons. D: The time courses and maximal effects of bath application of 10 nM and 100 nM N/OFQ were similar. E: Concentration response relationship for VTA neurons showing a positive change, both significant and not significant, in holding current with N/OFQ application (grey dots include all neurons with a change > 0 pA; median shown in white dots; black bars show 25 and 75 percentiles; 1 nM: n = 1/6; 10 nM: n = 55/86; 100 nM: n = 20/25; 1 μM: n = 7/7; 10 μM: n = 3/3).

239
240 To confirm responses were due to activation of the NOP, we tested whether these
241 inhibitions were blocked by the selective NOP antagonist BTRX-246040. In neurons responding
242 to N/OFQ with an outward current (10 nM mean response = 14 ± 3 pA) BTRX-246040 (100 nM)
243 was applied for 10 min and then N/OFQ was applied again in the presence of the antagonist.
244 BTRX-246040 consistently and completely blocked N/OFQ-induced outward currents (baseline
245 N/OFQ response: 14 ± 3 pA; N/OFQ response in BTRX-246040: -1 ± 2 pA; n = 15; 14 rats;
246 paired t-test: $p$ = 0.0005; Fig. 2).
247

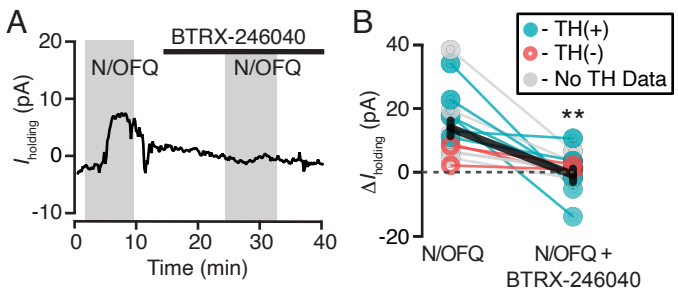


**Figure 2: BTRX-246040 consistently blocks N/OFQ induced currents.** A: Example recording of a N/OFQ (10 nM) responsive neuron where the selective NOP antagonist BTRX-246040 (100 nM) blocked the response to a subsequent N/OFQ application. B: BTRX-246040 blocked N/OFQ responses across VTA neurons, including both TH(+) and TH(-) neurons (n = 6 and 3, respectively; n = 6 no TH data; mean ± SEM in black). $^{**}P < 0.01$.

We also observed a subpopulation of neurons that responded to N/OFQ application with a small inward current, consistent with an excitatory effect (10 nM mean response = -16 ± 6 pA) (Fig. 3A,B). Inward currents were observed in approximately 25% (15/60) of the neurons that were responsive to N/OFQ (10 nM) and 17% of all 10 nM-tested VTA neurons (15/86; 15 neurons from 14 rats; Fig. 3C,D). Among 5 neurons responding to N/OFQ with an inward current and immunocytochemically identified, 40% (2/5) were TH(+) and 60% (3/5) were TH(-) (two tailed permutation test: $p = 0.6$; Fig. 3E). These N/OFQ evoked excitatory responses were only observed at low concentrations (< 100 nM; Fig. 3D); at higher concentrations only outward currents were observed (Fig. 1E, 3D). The neurons showing this excitatory response to N/OFQ were topographically intermixed with VTA neurons that responded to N/OFQ with an outward current (Fig. 3F).

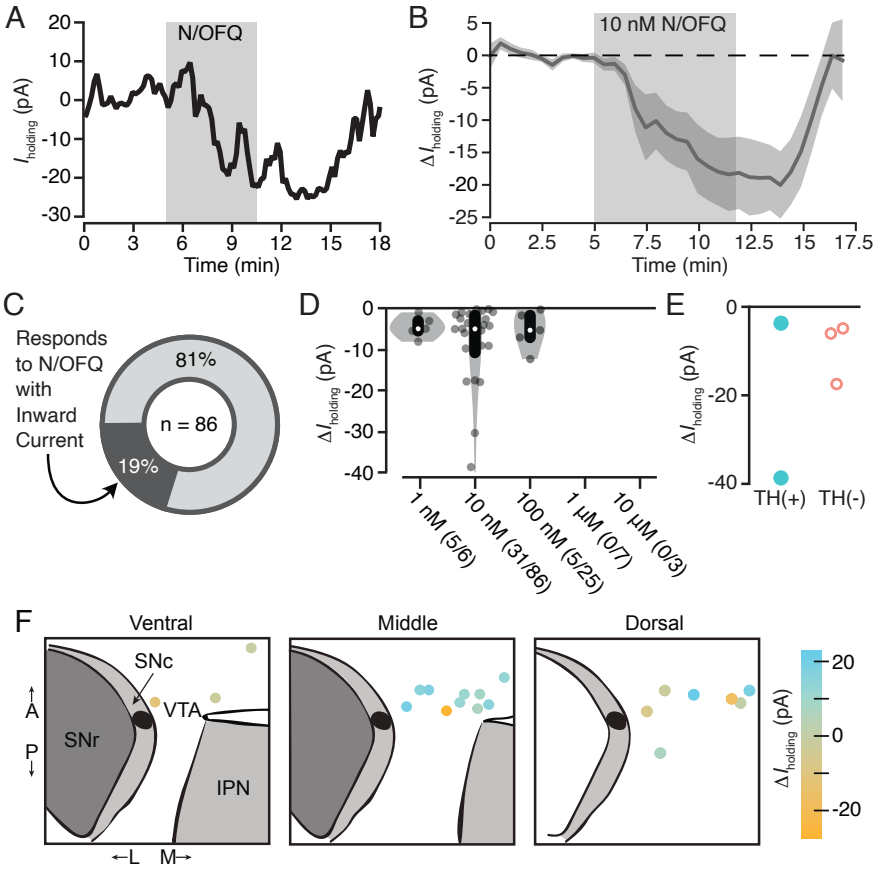


**Figure 3: Low dose N/OFQ induced small inward currents in a subset of VTA neurons.** A: Example voltage clamp recording ($V_{clamp}$ = -60 mV) of a VTA neuron that responded to N/OFQ with an inward current. B: The mean ± SEM time course across neurons with inward currents shows the onset of this response is time locked to the initiation of drug application (n = 13). C: Across all VTA neurons from control rats that were tested for 10 nM N/OFQ responses, 19% responded with a significant inward current. D: Grey dots indicate each neuron showing a negative change, both significant and not significant, in holding current with N/OFQ application (grey dots include all neurons with a change < 0 pA; median shown in white dots; black bars show 25 and 75 percentiles. Significant inward currents were observed at 10 nM, while higher concentrations only generated outward currents (see Fig. 1E). E: Inward currents were observed in both immunocytochemically identified TH(+) and TH(-) neurons. F: Locations of VTA recordings show that neurons that responded to N/OFQ with inward and outward currents were intermixed.

*Concentration dependent desensitization of NOP*

Given the inconsistencies in the reports of behavioral effects of NOP agonists and antagonists, we tested whether N/OFQ causes rapid NOP desensitization at moderate doses. We observed a concentration-dependent diminished response to a second application of N/OFQ when the first application of N/OFQ was ≥ 100 nM (n = 12 neurons from 12 rats; paired t-test $p$ = 0.00003; Fig. 4A,B). This is consistent with NOP desensitization, and observed in both TH(+) and TH(-) neurons (Fig. 4B). In contrast, following administration of 10 nM N/OFQ, no difference in response was observed between the first and second applications (n = 10 neurons from 8 rats; paired t-test $p$ = 0.13; Fig. 4C,D). Therefore, desensitization occurs at moderate N/OFQ concentrations in the VTA.

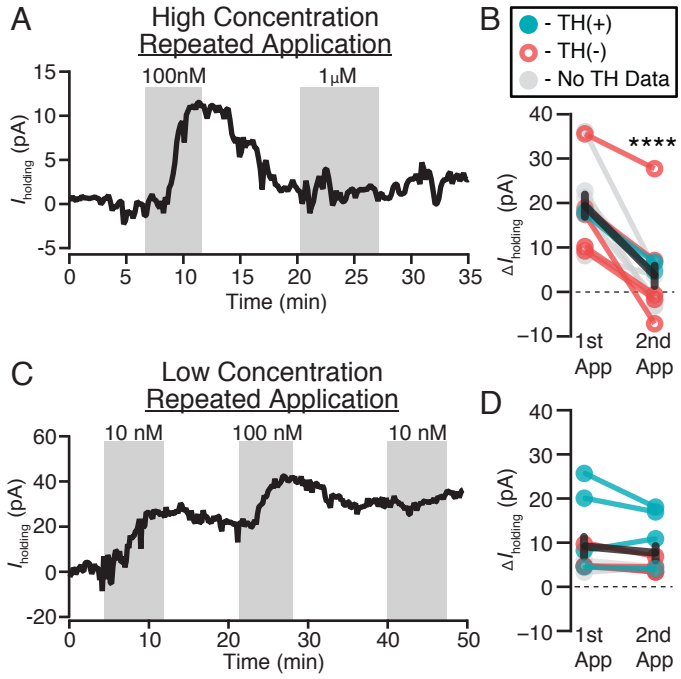


**Figure 4: Moderate doses of N/OFQ cause functional desensitization in VTA neurons.** A: Example voltage clamp recording ($V_{clamp}$ = -60 mV) where 100 nM is sufficient to prevent a subsequent response to 1 μM application of N/OFQ. B: A summary across VTA neurons where the first N/OFQ application was ≥ 100 nM, the response to the second application was consistently smaller (****$p$ = 0.00003), in both TH(+) and TH(-) neurons (n = 2 and 5, respectively; n = 5 no TH data). C: Example voltage clamp recording ($V_{clamp}$ = -60 mV) showing that 10 nM N/OFQ does not impair responses to subsequent N/OFQ application. In the same cell, 100 nM did prevent additional responding. D: Summary across VTA neurons shows similar magnitudes of responses to the second application of N/OFQ when the first application was 10 nM ($p$ = 0.13; TH(+) n = 4, TH(-) n = 2, TH no data n = 2).

*N/OFQ inhibits VTA neurons and SNc neurons via different cellular mechanisms*

We investigated the mechanism underlying the outward currents produced by N/OFQ in VTA neurons. The most common mechanism by which Gi/o coupled receptors, including the NOP, generate somatodendritic inhibition is by activation of GIRKs. First we tested if the $K^+$ channel blocker $BaCl_2$ (100 μM) prevented N/OFQ induced outward currents. Surprisingly, $BaCl_2$ did not prevent the outward currents induced by N/OFQ at either 100 nM (Fig. 5A) or 10 nM (Fig. 5B; one tailed permutation analysis comparing all 10 nM N/OFQ VTA observations (n = 86) to 10 nM N/OFQ observations in the presence of 100 μM $BaCl_2$ (n = 7), $p$ = 0.2). We next tested if a cocktail of synaptic blockers including the $Na^+$ channel blocker tetrotodoxin (500 nM), the α-amino-3-hydroxy-5-methyl-4-isoxazolepropionic acid receptor (AMPAR) blocker 6,7-dinitroquinoxaline-2,3(1H,4H)-dione (DNQX; 10 μM), and the $GABA_AR$ antagonist bicuculline (10 μM) would alter the distribution of N/OFQ responses (Fig. 5C). Interestingly, while this cocktail did not significantly change the mean of VTA neuron N/OFQ responses (two tailed permutation analysis comparing the means of all 10 nM N/OFQ VTA observations (n = 86) to 10

nM N/OFQ observations in the synaptic blocker cocktail (n = 9), $p$ = 0.16), the standard deviation of the distribution of N/OFQ responses in the presence of the inhibitor cocktail was significantly reduced, suggesting this treatment did diminish N/OFQ responses (one tailed permutation analysis comparing the standard deviations of all 10 nM N/OFQ VTA observations (n = 86) to 10 nM N/OFQ observations in the synaptic blocker cocktail (n = 9), $p$ = 0.03). Since the cocktail of synaptic blockers did not yield a significant change in the mean of the responses, this indicated that both outward and inward current responses were likely diminished, and inspection of the distribution indicates that in particular the N/OFQ induced outward currents were mostly prevented by this treatment (Fig. 5C). This raised the possibilities that the outward currents are via an inhibition of AMPAR signaling, via an increase in $GABA_AR$ signaling, or via a non-GIRK-dependent effect of a substance released by action potential activity in the slice. We previously found that in stressed animals, DOP activation in the VTA postsynaptically increases $GABA_AR$ signaling in VTA neurons (Margolis et al., 2011), while spontaneous glutamate release in the VTA seems insufficient to support generating an outward current by inhibiting glutamate release (Koga and Momiyama, 2000; Margolis et al., 2005; Xiao et al., 2008). In order to test whether N/OFQ affects $GABA_AR$ signaling in the VTA, and whether this might account for N/OFQ induced changes in holding current, we iontophoretically applied GABA in the presence of $GABA_BR$ blockade (CGP35348, 30 μM) to measure $GABA_AR$ responses and to bypass any potential presynaptic terminal effects. We not only found that 100 nM N/OFQ increased the amplitude of $GABA_AR$ responses (Fig. 5D,E), the effect on iontophoresed GABA currents was proportional to the change in holding current induced by N/OFQ (Fig. 5E), across both inward and outward currents induced by N/OFQ, making it likely that $GABA_AR$ signaling underlies both inward and outward currents induced by N/OFQ application to VTA neurons.

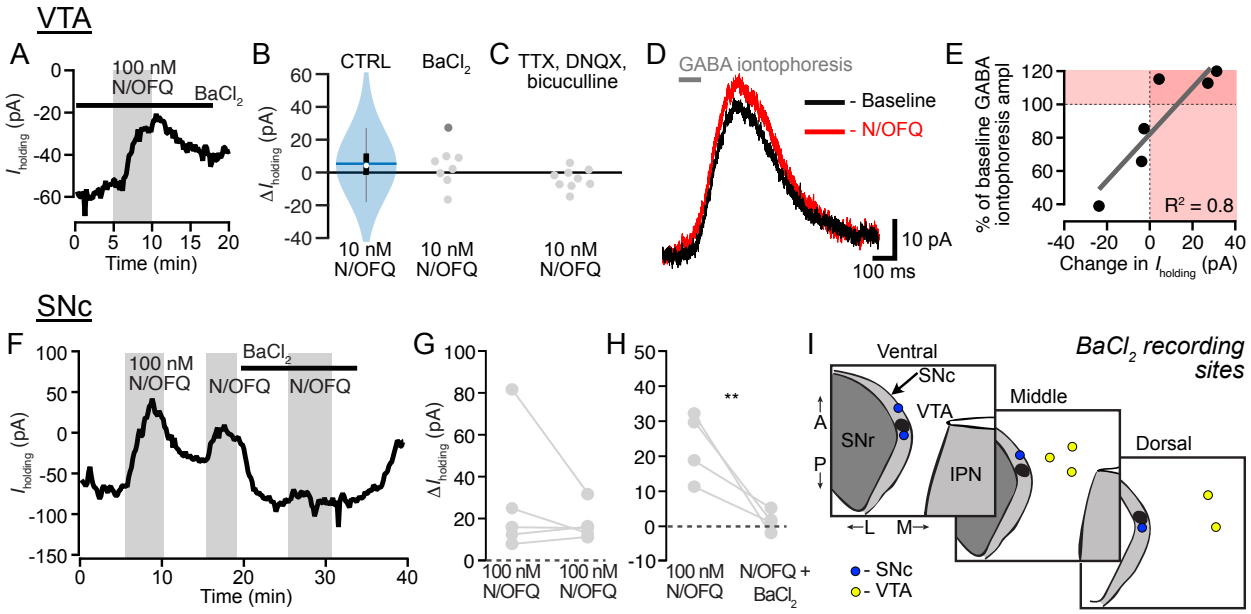

**Figure 5: $GABA_A$Rs, rather than GIRKs, mediate N/OFQ effects in VTA neurons**. A: Example recording showing that the $K^+$ channel blocker $BaCl_2$ (100 μM) did not prevent a N/OFQ induced outward current in a VTA neuron. B: Blue violin plot represents the distribution of responses of VTA neurons to 10 nM N/OFQ (blue horizontal line = mean; white circle = median; black rectangle = 25 and 75 percentiles). In comparison, gray circles showing responses to 10 nM N/OFQ (single 100 nM experiment in dark gray) in the presence of $BaCl_2$ have a similar distribution (one tailed permutation analysis of the means, $p = 0.2$). C: Recordings in 500 nM TTX, 10 μM DNQX, and 10 μM bicuculline, to block synaptic activity, AMPARs, and $GABA_A$Rs, respectively, showed an almost complete elimination of outward currents in VTA neurons in response to N/OFQ (two tailed permutation analysis of the means, $p = 0.16$; one tailed permutation analysis of the standard deviations, $p = 0.03$). D: Example recording of $GABA_A$R mediated iontophoretic responses to GABA (in 30 μM CGP35348 to block $GABA_B$Rs), showing an augmentation of response amplitude in response to 100 nM N/OFQ. E: Summary of the N/OFQ (100 nM) induced change in iontophoretic response vs change in $I_{holding}$, showing both inward and outward N/OFQ induced currents are highly correlated with N/OFQ induced changes in iontophoresis amplitude. F: Example recording in a SNc neuron showing repeated responses to high concentration (100 nM) N/OFQ, and complete blockade of the N/OFQ response by $BaCl_2$. G: Summary data from SNc neurons showing minimal desensitization in control experiments with repeated within cell N/OFQ applications at high concentration. H: Summary data from SNc neurons shows that $BaCl_2$ prevents a second response to N/OFQ, indicating that in the SNc, N/OFQ outward currents are mediated by $K^+$ channels, unlike VTA neurons. $^{**}p < 0.01$. I: Recording locations for VTA and SNc recordings where N/OFQ was tested in the presence of $BaCl_2$.

That N/OFQ induced outward currents are due to augmentations of $GABA_A$R mediated current rather than activation of a $K^+$ current was particularly surprising because it was previously reported that N/OFQ activates a $K^+$ channel in VTA neurons (Zheng et al., 2002). Zheng and colleagues also reported larger average outward currents compared to our dataset and did not observe desensitization with repeated applications of 300 nM N/OFQ, inconsistent with our findings here. As a positive control to test that 100 μM $BaCl_2$ was sufficient to block $K^+$ mediated effects in our preparation, and in an attempt to resolve these discrepancies, we completed additional recordings in the SNc, just lateral to the VTA (Fig. 5I). First, we tested if repeated application of 100 nM N/OFQ to SNc neurons resulted in less desensitization than we observed in VTA neurons. In fact, the response to the second 100 nM N/OFQ application was not statistically different from the response to the first application in SNc neurons, in contrast to VTA neurons (Fig. 5F,G; two-tailed paired t-Test, $p = 0.5$, n = 5). Therefore we used a within cell design to compare the N/OFQ response in control aCSF and in 100 μM $BaCl_2$. Blocking $K^+$ channels completely blocked the N/OFQ responses in SNc neurons (Fig. 5H; one-tailed paired t-test, $p = 0.003$, n = 5). Together, these observations indicate that $BaCl_2$ was fully capable of blocking GIRK mediated N/OFQ effects in our recording conditions, and suggest that the differences between our observations and those previously reports may be related to recording location (Fig. 5I).

*N/OFQ effects on VTA neurons vary with projection target*

As described above, we observed heterogeneity in responses of VTA neurons to N/OFQ. Given that other pharmacological responses of VTA neurons, including to KOP activation (Ford et al., 2006; Margolis et al., 2006) vary with projection target, we investigated whether the N/OFQ responses would be more consistent within subpopulations of VTA neurons that share a projection target. Accordingly, we recorded N/OFQ (10 nM) responses in VTA neurons that were retrogradely labeled by tracer injections into mPFC, pACC, or medial NAc (Fig. 6A,B). Recordings were conducted with the investigator blinded to the injection site.

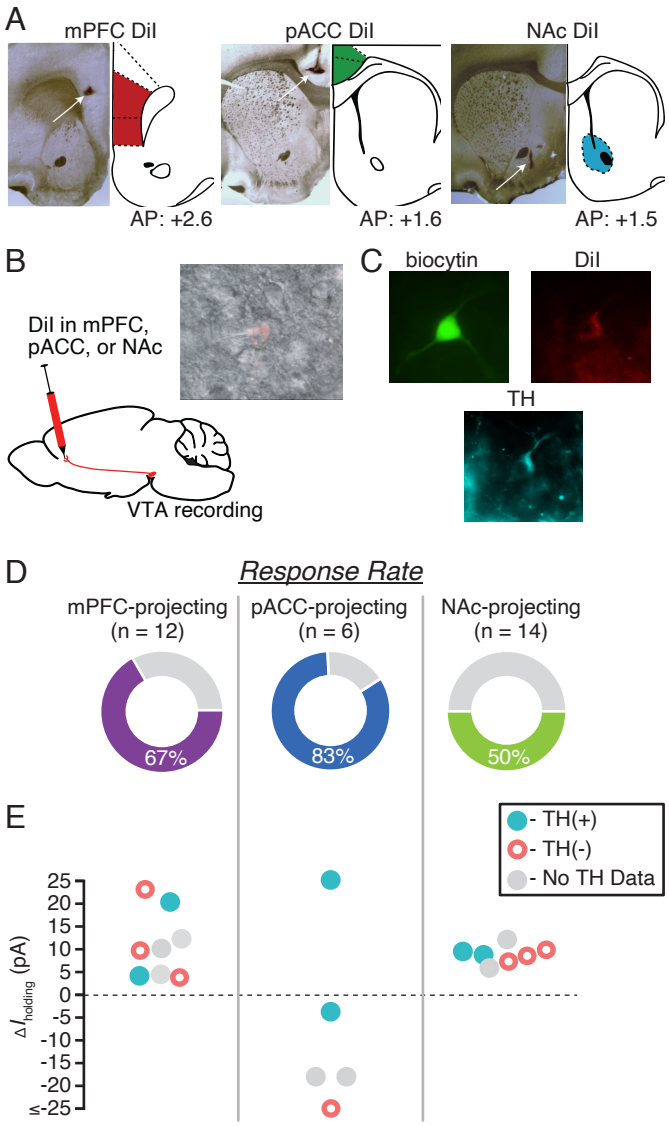


**Figure 6: N/OFQ effects in VTA neurons vary with projection target.** A: For each retrograde tracer injection site, example histology photo showing DiI localization (left) and mirrored, modified rat brain atlas schematic (right) (Paxinos and Watson, 1997). B: Cartoon showing the experimental approach: 7 days prior to recording, the retrograde tracer DiI was stereotaxically injected into mPFC, pACC, or medial NAc. DiI neurons were identified during whole cell recordings (inset). C: Example image of a neuron filled with biocytin during recording (green), the retrograde tracer (red) and was immunocytochemically identified as TH(+) (turquoise). D: The overall percentage of neurons that responded to N/OFQ was greatest among pACC-projecting neurons and lowest among NAc-projecting neurons. E: Graph of magnitudes of significant N/OFQ responses, showing that only pACC-projecting neurons respond to N/OFQ with an inward current.

The majority of mPFC-projecting VTA neurons, 67% (8/12), were significantly inhibited by N/OFQ, responding with an outward current (11 $\pm$ 3 pA; 8 responsive neurons from 6 rats; Fig. 6D). No N/OFQ induced inward currents were observed in mPFC-projecting neurons. Five mPFC-projecting neurons were recovered and processed for TH immunoreactivity (Fig. 6C,D); two were TH(+), and 3 were TH(-); all of these responded to N/OFQ with an outward current (Fig. 6D).

VTA projections to different cortical targets, including the pACC, arise from largely separate VTA neurons (Chandler et al., 2013). The pACC-projecting neurons are concentrated in different parts of the VTA, and fewer of them are dopaminergic compared to the projection to mPFC (Breton et al., 2019). Interestingly, 67% of the VTA neurons comprising this projection responded to N/OFQ with an inward current (4/6 inward current, -24 $\pm$ 12 pA, 1/6 outward current, from 4 rats; Fig. 6D). These N/OFQ excited, pACC-projecting VTA neurons included both TH(+) and TH(-) cells (Fig. 6D).

372 Half of NAc-projecting VTA neurons (7/14) responded to N/OFQ with outward currents (9
373 ± 1 pA, 7 responsive neurons from 7 rats; Fig. 6D). No inward currents were observed in this
374 projection. Of the 7 NAc-projecting neurons that responded to N/OFQ, 2 were confirmed TH(+)
375 and 3 were TH(-) (Fig. 6D). Together, these data indicate that similar N/OFQ inhibitory effects
376 occur in VTA neurons that project to mPFC and NAc, but these effects are opposed to those on
377 VTA projections to pACC, many of which responded to N/OFQ with an inward current.
378
379 *N/OFQ has little effect on terminal dopamine release in the NAc*
380 ICV or intra-VTA N/OFQ decreases dopamine levels in the NAc (Murphy et al., 1996;
381 Murphy and Maidment, 1999). Consistent with this result, we found that N/OFQ directly inhibits
382 a subset of the VTA dopamine NAc-projecting somata. N/OFQ may also inhibit dopamine
383 release in the NAc at the terminals; to test if NOPs on dopamine terminals in the NAc also
384 contribute to an N/OFQ-induced decrease in NAc dopamine levels, we used FSCV to detect
385 changes in stimulated dopamine release in NAc slices (Fig. 7A). In tissue from control SD rats
386 (9 rats), we stimulated dopamine release with a bipolar electrode. In a second set of animals, to
387 limit stimulation to dopaminergic axons, we expressed ChR2 in Th::Cre rats and stimulated with
388 470 nm light pulses (9 rats). In these preparations, repeated electrical, and especially optical,
389 stimulation can cause rundown in evoked dopamine release over time (Bass et al., 2013; O'Neill
390 et al., 2017). To minimize this rundown as much as possible, we increased the intervals
391 between light stimulations to 3 min. Where recordings were stable, effects of 10 nM N/OFQ, 100
392 nM N/OFQ, and 1 μM U69593 were sequentially tested. At 10 nM N/OFQ, approximately the
393 $EC_{50}$ of the outward currents recorded at VTA somata, there was no change in the peak FSCV
394 response to either electrical or light evoked dopamine release (electrically evoked dopamine
395 release: 93 ± 4% of baseline, n = 9 slices from 9 rats: linear mixed effects model, z = -1.3, $p$ =
396 0.2; optically evoked dopamine release: 94 ± 10% of baseline, n = 5 from 5 rats: linear mixed
397 effects model, z = -0.5, $p$ = 0.6; Fig. 7A,B). We detected a small but significant decrease in
398 evoked dopamine release in response to 100 nM N/OFQ (electrically evoked dopamine release:
399 88 ± 7% of baseline, n = 11 from 9 rats: linear mixed effects model, z = -2.1, $p$ = 0.04; optically
400 evoked dopamine release: 74 ± 4% of baseline, n = 17 from 9 rats: linear mixed effects model,
401 z = -7.2, $p$ < 0.001; Fig. 7B). Consistent with previous studies (Bass et al., 2013; O'Neill et al.,
402 2017), it is possible that this small decrease was driven, at least in part, by rundown of ChR2-
403 driven dopamine release. As a positive control, we applied the selective KOP agonist U69,593
404 (1 μM), previously shown to inhibit dopamine release in the NAc (G Di Chiara and Imperato,
405 1988; Ebner et al., 2010; Karkhanis et al., 2016; Spanagel et al., 1992; Werling et al., 1988), at
406 the end of each experiment, on top of N/OFQ since these drug responses were minimal.
407 U69,593 caused a substantial decrease in stimulated dopamine release (electrical: 53 ± 5% of
408 baseline (in N/OFQ), n = 15: linear mixed effects model, z = -8.9, $p$ < 0.001; optical: 49 ± 3% of
409 baseline (in N/OFQ), n = 17: linear mixed effects model, z = -13.9, $p$ < 0.001; Fig. 7B).
410 Therefore, the direct NOP modulation of this dopaminergic circuit occurs at a lower
411 concentration and may be stronger in the somadendritic region where the terminals in the NAc
412 are relatively insensitive to NOP activation. These results contrast with the KOP control of these
413 neurons, which strongly inhibits release at the NAc dopamine terminals but does not directly
414 hyperpolarize the cell bodies of these neurons (Margolis et al., 2006) (Fig. 7C).
415

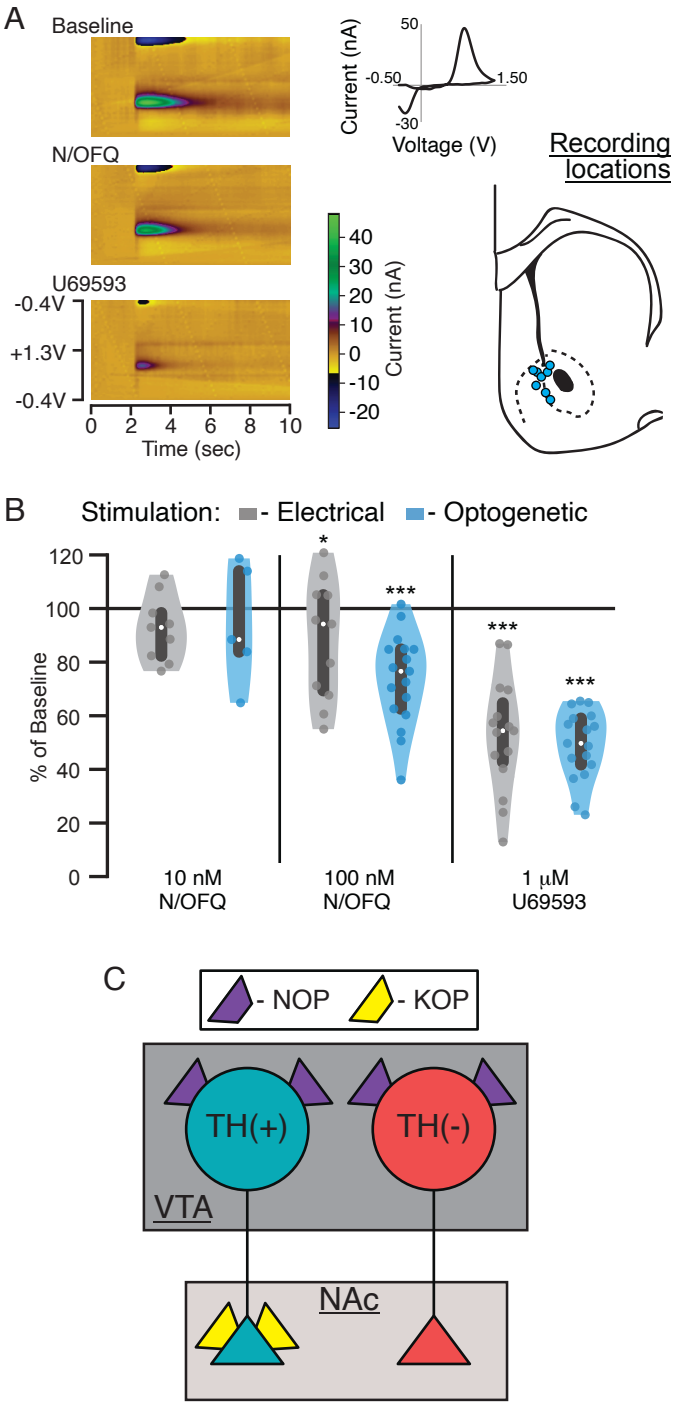


**Figure 7: N/OFQ does not inhibit dopamine release at NAc terminals.** We used FSCV in acute, coronal slices containing the NAc to test for N/OFQ effects on terminal release of dopamine. Dopamine release was evoked in slices from control rats with bipolar electrodes locally in the NAc. Recordings were made on the NAc shell-core border. Alternatively, to limit stimulation to dopamine fibers, Th::Cre rats were injected with (AAV2-Ef1a-DIO-hChR2(H134R)-mCherry) in the VTA at least 4 weeks prior to recordings, during which 470 nm light pulses were used to stimulate dopamine release. A: Example color plots of FSCV measurement of electrically evoed dopamine release. Inset, top: background subtracted cyclic voltammogram at peak of putative dopamine release. Inset, bottom: locations of FSCV recordings in schematic of coronal section of rat brain AP: +1.5 mm (Paxinos and Watson, 1997). B: Either 10 nM or 100 nM N/OFQ was applied to the slice; each on average had minimal effects on either electrically or light evoked dopamine release in the NAc. Following N/OFQ measures, without washout, we added the KOP agonist U69593 (1 μM), which inhibited evoked dopamine release. White dots represent median values and grey bars represent 25 and 75 percentiles. C: Summary diagram shows the contrast between NOP and KOP function in NAc-projecting VTA dopamine neurons. While NOP activation inhibits the somatodendritic compartment only, KOP induced inhibition is limited to dopaminergic axon terminals in these neurons. Further, NOP activation inhibits NAc-projecting non-dopaminergic VTA cell bodies, which are insensitive to KOP activation.

## Discussion

The results presented here demonstrate that N/OFQ affects both dopaminergic and non-dopaminergic VTA neurons, through activation of the NOP, and in the majority of neurons causes inhibitory outward currents. N/OFQ effects in these neurons were blocked by the NOP selective antagonist BTRX-246040, confirming its action at NOP. Importantly, neuronal responses to N/OFQ in VTA neurons desensitized at concentrations ≥ 100 nM. In addition to

424 providing a basic characterization of the range of postsynaptic N/OFQ responses in VTA
425 neurons, we demonstrated differential responding of subsets of VTA neurons to NOP activation
426 related to projection target: mPFC-projecting and NAc-projecting VTA neurons responded to
427 N/OFQ with outward currents (inhibitory), while most pACC-projecting VTA neurons responded
428 with inward currents (excitatory). Within the dopaminergic projection to the NAc, although
429 N/OFQ caused outward currents at the somatodendritic region of these neurons, release at the
430 terminals was not inhibited by NOP activation. Together, these data show that N/OFQ effects in
431 VTA neurons differ depending upon their projection target, and that at higher concentrations of
432 N/OFQ only inhibitions are observed, followed by desensitization of NOP function.
433 Unexpectedly, a small population of neurons in the VTA, both TH(+) and TH(-),
434 responded to low concentrations of N/OFQ with an inward current, consistent with excitation.
435 This finding presents a novel mechanism by which N/OFQ could selectively activate specific
436 VTA circuits, while inhibiting the majority of VTA outputs. Inward currents were observed in
437 most VTA neurons projecting to the pACC, but not those projecting to the NAc or mPFC,
438 consistent with this circuit-selection proposition. The fact that this effect was only observed at
439 low concentrations indicates that very robust N/OFQ release into the VTA, on the other hand,
440 would likely have a broad inhibitory effect on the vast majority of VTA neurons, regardless of
441 circuit. Although NOPs are generally thought to couple to Gi/o and inhibit neural activity, some
442 exceptions to this coupling have been reported for the related opioid receptors. Activation of
443 postsynaptic MOP or DOP results in a $Ca_v2.1$ channel-dependent depolarization in subsets of
444 VTA neurons (Margolis et al., 2017, 2014). Further, the MOP agonist DAMGO increases $Ca_v2.1$
445 currents in cerebellar Purkinje neurons (Iegorova et al., 2010) and morphine activates adenylyl
446 cyclase in the corpus striatum and olfactory bulb (Onali and Olianas, 1991; Puri et al., 1975).
447 While this is the first report of N/OFQ-mediated excitations in an acute brain slice preparation,
448 intracellular increases in $Ca^{2+}$ have been observed in a cultured human neuroblastoma cell line
449 in response to N/OFQ in the presence of the cholinergic agonist carbachol (Connor et al., 1996).
450 Therefore, while there are few reports of excitatory actions of N/OFQ, the observation is not
451 unprecedented.
452 We also found that NOP activation signals through the canonical GIRK pathway in the
453 SNc, however, in the VTA N/OFQ outward currents were mediated by augmentation of $GABA_AR$
454 currents. While both mechanisms generated outward currents in our experimental preparation,
455 the physiological consequences of these neural populations utilizing different signaling
456 pathways *in vivo* may vary. For instance, activating a GIRK will always cause a
457 hyperpolarization, while increasing the $GABA_AR$ current will only occur when there is concurrent
458 activation of NOPs and $GABA_ARs$. Further, the N/OFQ induced inhibition requiring $GABA_AR$
459 activation depends upon the $Cl^-$ reversal potential, which may be altered by a variety of
460 behavioral states including pain, morphine treatment, stress, or alcohol (Coull et al., 2003;
461 Ferrini et al., 2013; Hewitt et al., 2009; Ostroumov et al., 2016; Santos et al., 2017). The N/OFQ
462 response may even be excitatory in the absence of $GABA_AR$ activation, since blocking
463 $GABA_ARs$ seemed to increase the proportion of neurons in which we observed inward currents
464 in response to N/OFQ (Fig. 5C).
465 In the VTA, neurons treated with a higher concentration of N/OFQ ($\geq$ 100 nM) no longer
466 responded to subsequent applications of N/OFQ in the VTA. This finding indicates that N/OFQ
467 may act as a functional antagonist at the NOP by desensitizing these responses when higher

468 concentrations of N/OFQ are present. Interestingly, we did not observe significant NOP
469 desensitization in SNc neurons. NOP function is therefore apparently different from postsynaptic
470 responses to agonists at the MOP and DOP in VTA neurons, where repeated application of
471 saturating concentrations of selective agonists generate responses of similar magnitudes
472 (Margolis et al., 2017, 2014). The apparent NOP desensitization we observed in the VTA is
473 consistent with previous studies showing that high concentrations or repeated sustained
474 exposure to NOP agonists causes desensitization in cell culture (Connor et al., 1996; Mandyam
475 et al., 2002, 2000; Thakker and Standifer, 2002). In addition, NOPs internalize fairly rapidly
476 (Corbani et al., 2004; Spampinato et al., 2002, 2001; Zhang et al., 2012) at the same
477 concentrations that we observed desensitization. *In vivo*, N/OFQ administration can result in
478 dose dependent performance changes in behavioral spatial memory, locomotor, and anxiety
479 tasks, with low concentration N/OFQ having the opposite effects compared to high doses (Florin
480 et al., 1996; Jenck et al., 1997; Sandin et al., 2004). One possible explanation for these
481 opposing behavioral outcomes is that N/OFQ may be acting as an agonist at low concentrations
482 and a functional antagonist at high concentrations in some brain regions. An alternative
483 possibility is that brain regions like the SNc that have less desensization drive behavioral
484 responses to high doses of N/OFQ, where brain regions like the VTA that show more
485 desensitization do contribute to behavioral responses to lower N/OFQ doses.
486 N/OFQ inhibited both dopamine and non-dopamine neurons in the VTA that project to
487 the NAc. This finding is consistent with the observation that N/OFQ administered ICV or into the
488 VTA results in a decrease in extracellular dopamine in the NAc (Murphy et al., 1996; Murphy
489 and Maidment, 1999). A prominent proposal in the literature is that a decrease in NAc dopamine
490 produces aversion (McCutcheon et al., 2012). Therefore, one would expect ICV injection of
491 N/OFQ to be aversive. However, this manipulation generates no response in the place
492 conditioning paradigm (Devine et al., 1996). On the other hand, optogenetic or chemogenetic
493 stimulation of N/OFQ containing inputs to the VTA can be aversive and decrease reward
494 seeking (Parker et al., 2019). One possible explanation for this lack of clear motivational effect
495 is the combination of inhibition of both dopamine and non-dopamine neurons: dopamine and
496 non-dopamine neurons originating in the VTA synapse onto different types of neurons in the
497 NAc, therefore affecting behavior in different ways. For instance, VTA glutamate neurons
498 synapse onto parvalbumin containing interneurons in the NAc and optogenetic activation of
499 these NAc-projecting glutamate neurons is aversive (Qi et al., 2016). Activation of NAc-
500 projecting VTA GABA neurons causes a pause in cholinergic interneuron activity (Brown et al.,
501 2012). These neurons modulate associative learning but are insufficient to drive preference or
502 aversion independently (Collins et al., 2019) and do not appear to contribute to the detection of
503 aversive gustatory stimuli (Robble et al., 2020). N/OFQ inhibition of dopamine, GABA, and
504 glutamate neurons projecting to the NAc, therefore, may result in no net hedonic value and a
505 lack of preference in a place preference paradigm. Further, various reports indicate that
506 decreasing activity at dopamine receptors in the NAc with microinjections of antagonists does
507 not produce aversion (Baker et al., 1998, 1996; Fenu et al., 2006; Josselyn and Beninger, 1993;
508 Laviolette and van der Kooy, 2003; Morutto and Phillips, 1998; Spina et al., 2006) but see
509 (Shippenberg et al., 1991), and aversive outcomes can even be observed following
510 manipulations that increase dopamine levels in the NAc (Devine et al., 1993b; Shippenberg and
511 Bals-Kubik, 1995). Add to this the N/OFQ effects on other circuits following ICV injection,

512 including other VTA neurons, and the possibility that the most robust, long lasting effect is
513 receptor desensitization at higher doses of agonist, together making it potentially less surprising
514 that ICV N/OFQ was not reported to generate aversion.
515 N/OFQ's effect on the VTA to NAc circuit provides an interesting point of comparison for
516 how the NOP may be functionally distinct from the structurally related KOP. *In vivo*, systemic or
517 ICV administration of N/OFQ or a KOP agonist each causes a decrease in extracellular
518 dopamine in the NAc (Devine et al., 1993a; G. Di Chiara and Imperato, 1988; Murphy et al.,
519 1996; Murphy and Maidment, 1999). However, these two receptors function very differently in
520 the dopamine neurons that project to the NAc. We show here that N/OFQ inhibits VTA cell
521 bodies that project to the NAc, but has little effect on the dopamine terminals within the NAc.
522 Kappa opioid receptor activation, on the other hand, has no effect on the cell bodies of NAc-
523 projecting VTA dopamine neurons, but strongly inhibits dopamine release at the terminals in the
524 NAc (Britt and McGehee, 2008; Margolis et al., 2006) (Fig. 5C). One implication for this
525 organization is that whether or not the respective endogenous peptides, N/OFQ and dynorphin,
526 affect NAc-projecting dopamine neurons will depend upon the brain region of peptide release.
527 There is also evidence for dopamine release in the NAc that is independent of action potential
528 firing in midbrain dopamine neurons (Cachope et al., 2012; Mohebi et al., 2019). In this
529 organization of differential receptor effects localized to somadendritic regions vs terminals,
530 dynorphin has control over this terminal activity while N/OFQ does not. Together these
531 observations bring into focus the critical importance of understanding precisely where receptors
532 are functional in brain circuits and their specific actions at each site.
533 We found opposing effects of N/OFQ on the VTA projections to mPFC and pACC, which
534 may contribute to the reported N/OFQ impact on behavioral measures associated with cortical
535 dopamine function such as working memory, learning, and behavioral flexibility (Gonzalez et al.,
536 2014; Huang et al., 2018; Ott and Nieder, 2019; Puig et al., 2014; Tzschentke, 2001; Winter et
537 al., 2009). Our results also show that the non-dopamine VTA projection to cortical regions are
538 affected by N/OFQ as well; while the majority of the VTA neurons that project to these cortical
539 regions are not dopaminergic (Breton et al., 2019), little is currently known regarding their
540 contribution to behavior. Preclinical studies show that ICV administration of N/OFQ impairs
541 working memory (Hiramatsu and Inoue, 1999) and associative learning and memory (Goeldner
542 et al., 2009), and blocking NOP with an antagonist or genetic knockout enhances both working
543 memory and learning (Jinsmaa et al., 2000; Nagai et al., 2007; Noda et al., 1999). How and
544 why such an ongoing break on learning and memory by N/OFQ contributes to normal behavioral
545 adaptation, and whether dopamine or other VTA outputs play a role, remains to be determined.
546 One provocative possibility is that it is this degradation of working memory function that is the
547 primary mechanism underlying the lack of place conditioning in response to central N/OFQ,
548 rather than that this treatment is affectively neutral. This interpretation is consistent with work
549 showing that N/OFQ blocks opioid induced conditioned place preference yet has no effect on
550 opioid self-administration as well (Sakoori and Murphy, 2004; Walker et al., 1998).
551 The results of this study extend our understanding of the NOP system biology and
552 provide considerations for additional investigation into NOP function within limbic circuits.
553 These findings clarify that strong NOP desensitization occurs in neurons at moderate
554 concentrations of the endogenous agonist N/OFQ. Importantly, not only does the nature of the
555 NOP response vary with the projection target of VTA neurons, but the NOP function is largely

556 sequestered to the somatodendritic compartment of VTA dopamine neurons that project to the
557 NAc, demonstrating two different kinds of circuit level organization of this receptor system.
558 Building on this groundwork, future studies of these VTA circuits during different behavioral
559 states and tasks related to motivation and cognition will help to elucidate the differences
560 between the normal and dysfunctional NOP-N/OFQ system, improving the potential for
561 therapeutic targeting.
562
563 **References**


564 Baker DA, Fuchs RA, Specio SE, Khroyan TV, Neisewander JL (1998) Effects of intraaccumbens
565 administration of SCH-23390 on cocaine-induced locomotion and conditioned place
566 preference. Synapse 30:181–93.
567 Baker DA, Khroyan TV, O'Dell LE, Fuchs RA, Neisewander JL (1996) Differential effects of intra-
568 accumbens sulpiride on cocaine-induced locomotion and conditioned place preference.
569 J Pharmacol Exp Ther 279:392–401.
570 Bass CE, Grinevich VP, Kulikova AD, Bonin KD, Budygin EA (2013) Terminal effects of
571 optogenetic stimulation on dopamine dynamics in rat striatum. J Neurosci Methods
572 214:149–155.
573 Berthele A, Platzer S, Dworzak D, Schadrack J, Mahal B, Büttner A, Aßmus HP, Wurster K,
574 Zieglgänsberger W, Conrad B, Tölle TR (2003) [3h]-nociceptin ligand-binding and
575 nociceptin opioid receptor mrna expression in the human brain. Neuroscience 121:629–
576 640.
577 Breton JM, Charbit AR, Snyder BJ, Fong PTK, Dias EV, Himmels P, Lock H, Margolis EB (2019)
578 Relative contributions and mapping of ventral tegmental area dopamine and GABA
579 neurons by projection target in the rat. J Comp Neurol 527:916–941.
580 Britt JP, McGehee DS (2008) Presynaptic opioid and nicotinic receptor modulation of dopamine
581 overflow in the nucleus accumbens. J Neurosci 28:1672–1681.
582 Brown MT, Tan KR, O'Connor EC, Nikonenko I, Muller D, Lüscher C (2012) Ventral tegmental
583 area GABA projections pause accumbal cholinergic interneurons to enhance associative
584 learning. Nature 492:452–6.
585 Bunzow JR, Saez C, Mortrud M, Bouvier C, Williams JT, Low M, Grandy DK (1994) Molecular
586 cloning and tissue distribution of a putative member of the rat opioid receptor gene
587 family that is not a μ, δ or κ opioid receptor type. FEBS Letters 347:284–288.
588 Cachope R, Mateo Y, Mathur BN, Irving J, Wang HL, Morales M, Lovinger DM, Cheer JF (2012)
589 Selective activation of cholinergic interneurons enhances accumbal phasic dopamine
590 release: setting the tone for reward processing. Cell Rep 2:33–41.
591 Chandler DJ, Lamperski CS, Waterhouse BD (2013) Identification and distribution of projections
592 from monoaminergic and cholinergic nuclei to functionally differentiated subregions of
593 prefrontal cortex. Brain Res 1522:38–58.

594 Ciccocioppo R, Angeletti S, Panocka I, Massi M (2000) Nociceptin/orphanin FQ and drugs of
595 abuse. Peptides 21:1071–1080.
596 Ciccocioppo R, Stopponi S, Economidou D, Kuriyama M, Kinoshita H, Heilig M, Roberto M, Weiss
597 F, Teshima K (2014) Chronic treatment with novel brain-penetrating selective NOP
598 receptor agonist MT-7716 reduces alcohol drinking and seeking in the rat.
599 Neuropsychopharmacology 39:2601–2610.
600 Civelli O (2008) The Orphanin FQ/Nociceptin (OFQ/N) System In: Orphan G Protein-Coupled
601 Receptors and Novel Neuropeptides, Results and Problems in Cell Differentiation (Civelli
602 O, Zhou Q-Y eds), pp1–25. Berlin, Heidelberg: Springer Berlin Heidelberg.
603 Collins AL, Aitken TJ, Huang I-W, Shieh C, Greenfield VY, Monbouquette HG, Ostlund SB,
604 Wassum KM (2019) Nucleus Accumbens Cholinergic Interneurons Oppose Cue-
605 Motivated Behavior. Biol Psychiatry.
606 Connor M, Yeo A, Henderson G (1996) The effect of nociceptin on Ca2+ channel current and
607 intracellular Ca2+ in the SH-SY5Y human neuroblastoma cell line. Br J Pharmacol
608 118:205–207.
609 Corbani M, Gonindard C, Meunier J-C (2004) Ligand-Regulated Internalization of the Opioid
610 Receptor-Like 1: A Confocal Study. Endocrinology 145:2876–2885.
611 Coull JAM, Boudreau D, Bachand K, Prescott SA, Nault F, Sík A, De Koninck P, De Koninck Y
612 (2003) Trans-synaptic shift in anion gradient in spinal lamina I neurons as a mechanism
613 of neuropathic pain. Nature 424:938–942.
614 Cox BM, Christie MJ, Devi L, Toll L, Traynor JR (2015) Challenges for opioid receptor
615 nomenclature: IUPHAR Review 9. Br J Pharmacol 172:317–323.
616 Dautzenberg FM, Wichmann J, Higelin J, Py-Lang G, Kratzeisen C, Malherbe P, Kilpatrick GJ,
617 Jenck F (2001) Pharmacological Characterization of the Novel Nonpeptide Orphanin
618 FQ/Nociceptin Receptor Agonist Ro 64-6198: Rapid and Reversible Desensitization of
619 the ORL1 Receptor in Vitro and Lack of Tolerance in Vivo. J Pharmacol Exp Ther
620 298:812–819.
621 Devine DP, Leone P, Pocock D, Wise RA (1993a) Differential involvement of ventral tegmental
622 mu, delta and kappa opioid receptors in modulation of basal mesolimbic dopamine
623 release: in vivo microdialysis studies. J Pharmacol Exp Ther 266:1236–46.
624 Devine DP, Leone P, Wise RA (1993b) Mesolimbic dopamine neurotransmission is increased by
625 administration of mu-opioid receptor antagonists. Eur J Pharmacol 243:55–64.
626 Devine DP, Reinscheid RK, Monsma FJ, Civelli O, Akil H (1996) The novel neuropeptide orphanin
627 FQ fails to produce conditioned place preference or aversion. Brain Research 727:225–
628 229.
629 Devine DP, Watson SJ, Akil H (2001) Nociceptin/orphanin FQ regulates neuroendocrine function
630 of the limbic–hypothalamic–pituitary–adrenal axis. Neuroscience 102:541–553.

631 Di Chiara G, Imperato A (1988) Drugs abused by humans preferentially increase synaptic
632 dopamine concentrations in the mesolimbic system of freely moving rats. Proc Natl
633 Acad Sci U S A 85:5274–5278.
634 Di Chiara G., Imperato A (1988) Opposite effects of mu and kappa opiate agonists on dopamine
635 release in the nucleus accumbens and in the dorsal caudate of freely moving rats. J
636 Pharmacol Exp Ther 244:1067–1080.
637 Di Giannuario A, Pieretti S (2000) Nociceptin differentially affects morphine-induced dopamine
638 release from the nucleus accumbens and nucleus caudate in rats. Peptides 21:1125–
639 1130.
640 Ebner SR, Roitman MF, Potter DN, Rachlin AB, Chartoff EH (2010) Depressive-like effects of the
641 kappa opioid receptor agonist salvinorin A are associated with decreased phasic
642 dopamine release in the nucleus accumbens. Psychopharmacology (Berl) 210:241–252.
643 Fenu S, Spina L, Rivas E, Longoni R, Di Chiara G (2006) Morphine-conditioned single-trial place
644 preference: role of nucleus accumbens shell dopamine receptors in acquisition, but not
645 expression. Psychopharmacology (Berl) 187:143–53.
646 Fernandez F, Misilmeri MA, Felger JC, Devine DP (2004) Nociceptin/Orphanin FQ Increases
647 Anxiety-Related Behavior and Circulating Levels of Corticosterone During Neophobic
648 Tests of Anxiety. Neuropsychopharmacology 29:59–71.
649 Ferrini F, Trang T, Mattioli TA, Laffray S, Del'Guidice T, Lorenzo LE, Castonguay A, Doyon N,
650 Zhang W, Godin AG, Mohr D, Beggs S, Vandal K, Beaulieu JM, Cahill CM, Salter MW, De
651 Koninck Y (2013) Morphine hyperalgesia gated through microglia-mediated disruption
652 of neuronal $Cl^-$ homeostasis. Nat Neurosci 16:183–92.
653 Fields HL, Hjelmstad GO, Margolis EB, Nicola SM (2007) Ventral tegmental area neurons in
654 learned appetitive behavior and positive reinforcement. Annu Rev Neurosci 30:289–316.
655 Florin S, Suaudeau C, Meunier J-C, Costentin J (1996) Nociceptin stimulates locomotion and
656 exploratory behaviour in mice. European Journal of Pharmacology 317:9–13.
657 Ford CP, Mark GP, Williams JT (2006) Properties and opioid inhibition of mesolimbic dopamine
658 neurons vary according to target location. J Neurosci 26:2788–97.
659 Gavioli EC, Rae GA, Calo' G, Guerrini R, De Lima TCM (2002) Central injections of nocistatin or its
660 C-terminal hexapeptide exert anxiogenic-like effect on behaviour of mice in the plus-
661 maze test. Br J Pharmacol 136:764–772.
662 Gintzler AR, Adapa ID, Toll L, Medina VM, Wang L (1997) Modulation of enkephalin release by
663 nociceptin (orphanin FQ). European Journal of Pharmacology 325:29–34.
664 Goeldner C, Reiss D, Wichmann J, Kieffer BL, Ouagazzal A-M (2009) Activation of nociceptin
665 opioid peptide (NOP) receptor impairs contextual fear learning in mice through
666 glutamatergic mechanisms. Neurobiol Learn Mem 91:393–401.

667 Gonzalez MC, Kramar CP, Tomaiuolo M, Katche C, Weisstaub N, Cammarota M, Medina JH
668 (2014) Medial prefrontal cortex dopamine controls the persistent storage of aversive
669 memories. Front Behav Neurosci 8.
670 Green MK, Barbieri EV, Brown BD, Chen K-W, Devine DP (2007) Roles of the bed nucleus of stria
671 terminalis and of the amygdala in N/OFQ-mediated anxiety and HPA axis activation.
672 Neuropeptides 41:399–410.
673 Green MK, Devine DP (2009) Nociceptin/Orphanin FQ and NOP receptor gene regulation after
674 acute or repeated social defeat stress. Neuropeptides 43:507–514.
675 Hawes BE, Graziano MP, Lambert DG (2000) Cellular actions of nociceptin: transduction
676 mechanisms. Peptides 21:961–967.
677 Hewitt SA, Wamsteeker JI, Kurz EU, Bains JS (2009) Altered chloride homeostasis removes
678 synaptic inhibitory constraint of the stress axis. Nat Neurosci 12:438–443.
679 Hiramatsu M, Inoue K (1999) Effects of nocistatin on nociceptin-induced impairment of learning
680 and memory in mice. Eur J Pharmacol 367:151–155.
681 Huang S, Borgland SL, Zamponi GW (2018) Dopaminergic modulation of pain signals in the
682 medial prefrontal cortex: Challenges and perspectives. Neuroscience Letters.
683 Iegorova O, Fisyunov A, Krishtal O (2010) G-protein-independent modulation of P-type calcium
684 channels by μ-opioids in Purkinje neurons of rat. Neurosci Lett 480:106–111.
685 Jenck F, Moreau J-L, Martin JR, Kilpatrick GJ, Reinscheid RK, Monsma FJ, Nothacker H-P, Civelli
686 O (1997) Orphanin FQ acts as an anxiolytic to attenuate behavioral responses to stress.
687 Proc Natl Acad Sci U S A 94:14854–14858.
688 Jinsmaa Y, Takahashi M, Fukunaga H, Yoshikawa M (2000) Retro-nociceptin methylester, a
689 peptide with analgesic and memory-enhancing activity. Life Sciences 67:3095–3101.
690 Josselyn SA, Beninger RJ (1993) Neuropeptide Y: intraaccumbens injections produce a place
691 preference that is blocked by cis-flupenthixol. Pharmacol Biochem Behav 46:543–52.
692 Kamei J, Matsunawa Y, Miyata S, Tanaka S, Saitoh A (2004) Effects of nociceptin on the
693 exploratory behavior of mice in the hole-board test. European Journal of Pharmacology
694 489:77–87.
695 Karkhanis AN, Rose JH, Weiner JL, Jones SR (2016) Early-Life Social Isolation Stress Increases
696 Kappa Opioid Receptor Responsiveness and Downregulates the Dopamine System.
697 Neuropsychopharmacology 41:2263–2274.
698 Kim KM, Baratta MV, Yang A, Lee D, Boyden ES, Fiorillo CD (2012) Optogenetic mimicry of the
699 transient activation of dopamine neurons by natural reward is sufficient for operant
700 reinforcement. PLoS ONE 7:e33612.
701 Knoflach F, Reinscheid RK, Civelli O, Kemp JA (1996) Modulation of Voltage-Gated Calcium
702 Channels by Orphanin FQ in Freshly Dissociated Hippocampal Neurons. J Neurosci
703 16:6657–6664.

704 Koga E, Momiyama T (2000) Presynaptic dopamine D2-like receptors inhibit excitatory
705 transmission onto rat ventral tegmental dopaminergic neurones. J Physiol (Lond) 523 Pt
706 1:163–173.
707 Kuzmin A, Kreek MJ, Bakalkin G, Liljequist S (2007) The nociceptin/orphanin FQ receptor agonist
708 Ro 64-6198 reduces alcohol self-administration and prevents relapse-like alcohol
709 drinking. Neuropsychopharmacology 32:902–910.
710 Laviolette SR, van der Kooy D (2003) Blockade of mesolimbic dopamine transmission
711 dramatically increases sensitivity to the rewarding effects of nicotine in the ventral
712 tegmental area. Mol Psychiatry 8:50–9, 9.
713 Leggett JD, Harbuz MS, Jessop DS, Fulford AJ (2006) The nociceptin receptor antagonist
714 [Nphe1,Arg14,Lys15]nociceptin/orphanin FQ-NH2 blocks the stimulatory effects of
715 nociceptin/orphanin FQ on the HPA axis in rats. Neuroscience 141:2051–2057.
716 Leggett JD, Jessop DS, Fulford AJ (2007) The nociceptin/orphanin FQ antagonist UFP-101
717 differentially modulates the glucocorticoid response to restraint stress in rats during the
718 peak and nadir phases of the hypothalamo–pituitary–adrenal axis circadian rhythm.
719 Neuroscience 147:757–764.
720 Lutfy K, Do T, Maidment NT (2001) Orphanin FQ/nociceptin attenuates motor stimulation and
721 changes in nucleus accumbens extracellular dopamine induced by cocaine in rats.
722 Psychopharmacology (Berl) 154:1–7.
723 Ma L, Cheng Z-J, Fan G-H, Cai Y-C, Jiang L-Z, Pei G (1997) Functional expression, activation and
724 desensitization of opioid receptor-like receptor ORL1 in neuroblastoma×glioma NG108-
725 15 hybrid cells. FEBS Letters 403:91–94.
726 Mandyam CD, Altememi GF, Standifer KM (2000) β-Funaltrexamine inactivates ORL1 receptors
727 in BE(2)-C human neuroblastoma cells. European Journal of Pharmacology 402:205–207.
728 Mandyam CD, Thakker DR, Christensen JL, Standifer KM (2002) Orphanin FQ/Nociceptin-
729 Mediated Desensitization of Opioid Receptor-Like 1 Receptor and μ Opioid Receptors
730 Involves Protein Kinase C: A Molecular Mechanism for Heterologous Cross-Talk. J
731 Pharmacol Exp Ther 302:502–509.
732 Margolis EB, Fujita W, Devi LA, Fields HL (2017) Two delta opioid receptor subtypes are
733 functional in single ventral tegmental area neurons, and can interact with the mu opioid
734 receptor. Neuropharmacology 123:420–432.
735 Margolis EB, Hjelmstad GO, Bonci A, Fields HL (2005) Both kappa and mu opioid agonists inhibit
736 glutamatergic input to ventral tegmental area neurons. J Neurophysiol 93:3086–93.
737 Margolis EB, Hjelmstad GO, Fujita W, Fields HL (2014) Direct Bidirectional μ-Opioid Control of
738 Midbrain Dopamine Neurons. J Neurosci 34:14707–14716.
739 Margolis EB, Lock H, Chefer VI, Shippenberg TS, Hjelmstad GO, Fields HL (2006) Kappa opioids
740 selectively control dopaminergic neurons projecting to the prefrontal cortex. Proc Natl
741 Acad Sci U S A 103:2938–42.

742 Margolis EB, Mitchell JM, Hjelmstad GO, Fields HL (2011) A novel opioid receptor-mediated
743 enhancement of GABAA receptor function induced by stress in ventral tegmental area
744 neurons. J Physiol 589:4229–42.
745 McCutcheon JE, Ebner SR, Loriaux AL, Roitman MF (2012) Encoding of aversion by dopamine
746 and the nucleus accumbens. Front Neurosci 6:137.
747 Meng F, Taylor LP, Hoversten MT, Ueda Y, Ardati A, Reinscheid RK, Monsma FJ, Watson SJ,
748 Civelli O, Akil H (1996) Moving from the Orphanin FQ Receptor to an Opioid Receptor
749 Using Four Point Mutations. J Biol Chem 271:32016–32020.
750 Meunier J-C, Mollereau C, Toll L, Suaudeau C, Moisand C, Alvinerie P, Butour J-L, Guillemot J-C,
751 Ferrara P, Monsarrat B, Mazarguil H, Vassart G, Parmentier M, Costentin J (1995)
752 Isolation and structure of the endogenous agonist of opioid receptor-like ORL1 receptor.
753 Nature 377:532–535.
754 Mogil JS, Pasternak GW (2001) The Molecular and Behavioral Pharmacology of the Orphanin
755 FQ/Nociceptin Peptide and Receptor Family. Pharmacol Rev 53:381–415.
756 Mohebi A, Pettibone JR, Hamid AA, Wong J-MT, Vinson LT, Patriarchi T, Tian L, Kennedy RT,
757 Berke JD (2019) Dissociable dopamine dynamics for learning and motivation. Nature.
758 Mollereau C, Parmentier M, Mailleux P, Butour JL, Moisand C, Chalon P, Caput D, Vassart G,
759 Meunier JC (1994) ORL1, a novel member of the opioid receptor family. Cloning,
760 functional expression and localization. FEBS Lett 341:33–38.
761 Morales M, Margolis EB (2017) Ventral tegmental area: cellular heterogeneity, connectivity and
762 behaviour. Nat Rev Neurosci 18:73–85.
763 Morutto SL, Phillips GD (1998) Interactions between sulpiride infusions within the perifornical
764 region of the lateral hypothalamus and the nucleus accumbens on measures of
765 locomotor activity and conditioned place preference. Behav Pharmacol 9:345–55.
766 Murphy NP, Ly HT, Maidment NT (1996) Intracerebroventricular orphanin FQ/Nociceptin
767 supresses dopamine release in the nucleus accumbens of anaesthetized rats.
768 Neuroscience 75:1–4.
769 Murphy NP, Maidment NT (1999) Orphanin FQ/Nociceptin Modulation of Mesolimbic
770 Dopamine Transmission Determined by Microdialysis. Journal of Neurochemistry
771 73:179–186.
772 Nagai J, Kurokawa M, Takeshima H, Kieffer BL, Ueda H (2007) Circadian-Dependent Learning
773 and Memory Enhancement in Nociceptin Receptor-Deficient Mice with a Novel
774 KUROBOX Apparatus Using Stress-Free Positive Cue Task. J Pharmacol Exp Ther
775 321:195–201.
776 Nativio P, Pascale E, Maffei A, Scaccianoce S, Passarelli F (2012) Effect of stress on hippocampal
777 nociceptin expression in the rat. Stress 15:378–384.
778 Neal CR, Mansour A, Reinscheid R, Nothacker HP, Civelli O, Akil H, Watson SJ (1999) Opioid
779 receptor-like (ORL1) receptor distribution in the rat central nervous system: comparison

780 of ORL1 receptor mRNA expression with (125)I-[(14)Tyr]-orphanin FQ binding. J Comp
781 Neurol 412:563–605.
782 New DC, Wong YH (2002) The ORL1 Receptor: Molecular Pharmacology and Signalling
783 Mechanisms. NSG 11:197–212.
784 Nicholson JR, Akil H, Watson SJ (2002) Orphanin FQ-induced hyperphagia is mediated by
785 corticosterone and central glucocorticoid receptors. Neuroscience 115:637–643.
786 Noda Y, Mamiya T, Nabeshima T (1999) [Behavioral pharmacological characterization of mice
787 lacking the nociceptin receptor]. Nihon Shinkei Seishin Yakurigaku Zasshi 19:73–78.
788 Onali P, Olianas MC (1991) Naturally occurring opioid receptor agonists stimulate adenylate
789 cyclase activity in rat olfactory bulb. Mol Pharmacol 39:436–441.
790 O'Neill B, Patel JC, Rice ME (2017) Characterization of Optically and Electrically Evoked
791 Dopamine Release in Striatal Slices from Digenic Knock-in Mice with DAT-Driven
792 Expression of Channelrhodopsin. ACS Chem Neurosci 8:310–319.
793 Ostroumov A, Thomas AM, Kimmey BA, Karsch JS, Doyon WM, Dani JA (2016) Stress Increases
794 Ethanol Self-Administration via a Shift toward Excitatory GABA Signaling in the Ventral
795 Tegmental Area. Neuron 92:493–504.
796 Ott T, Nieder A (2019) Dopamine and Cognitive Control in Prefrontal Cortex. Trends in Cognitive
797 Sciences 0.
798 Parker KE et al. (2019) A Paranigral VTA Nociceptin Circuit that Constrains Motivation for
799 Reward. Cell 178:653-671.e19.
800 Paxinos G, Watson C (1997) The Rat Brain in Stereotaxic Coordinates, Compact, 3rd ed. San
801 Diego: Academic Press.
802 Puig MV, Antzoulatos EG, Miller EK (2014) Prefrontal Dopamine in Associative Learning and
803 Memory. Neuroscience 282:217–229.
804 Puri SK, Cochin J, Volicer L (1975) Effect of morphine sulfate on adenylate cyclase and
805 phosphodiesterase activities in rat corpus striatum. Life Sciences 16:759–767.
806 Qi J, Zhang S, Wang HL, Barker DJ, Miranda-Barrientos J, Morales M (2016) VTA glutamatergic
807 inputs to nucleus accumbens drive aversion by acting on GABAergic interneurons. Nat
808 Neurosci 19:725–33.
809 Reinscheid RK, Ardati A, Monsma FJ, Civelli O (1996) Structure-Activity Relationship Studies on
810 the Novel Neuropeptide Orphanin FQ. J Biol Chem 271:14163–14168.
811 Reinscheid RK, Nothacker H-P, Bourson A, Ardati A, Henningsen RA, Bunzow JR, Grandy DK,
812 Langen H, Monsma FJ, Civelli O (1995) Orphanin FQ: A Neuropeptide That Activates an
813 Opioidlike G Protein-Coupled Receptor. Science 270:792–794.
814 Robble MA, Bozsik ME, Wheeler DS, Wheeler RA (2020) Learned avoidance requires VTA KOR-
815 mediated reductions in dopamine. Neuropharmacology 167:107996.
816 Rorick-Kehn LM, Ciccocioppo R, Wong CJ, Witkin JM, Martinez-Grau MA, Stopponi S, Adams BL,
817 Katner JS, Perry KW, Toledo MA, Diaz N, Lafuente C, Jiménez A, Benito A, Pedregal C,

818 Weiss F, Statnick MA (2016) A Novel, Orally Bioavailable Nociceptin Receptor
819 Antagonist, LY2940094, Reduces Ethanol Self-Administration and Ethanol Seeking in
820 Animal Models. Alcohol Clin Exp Res 40:945–954.
821 Sakoori K, Murphy NP (2004) Central administration of nociceptin/orphanin FQ blocks the
822 acquisition of conditioned place preference to morphine and cocaine, but not
823 conditioned place aversion to naloxone in mice. Psychopharmacology (Berl) 172:129–
824 136.
825 Sandin J, Ögren SO, Terenius L (2004) Nociceptin/orphanin FQ modulates spatial learning via
826 ORL-1 receptors in the dorsal hippocampus of the rat. Brain Research 997:222–233.
827 Santos LEC, Rodrigues AM, Lopes MR, Costa VDC, Scorza CA, Scorza FA, Cavalheiro EA, Almeida
828 A-CG (2017) Long-term alcohol exposure elicits hippocampal nonsynaptic epileptiform
829 activity changes associated with expression and functional changes in NKCC1, KCC2 co-
830 transporters and Na+/K+-ATPase. Neuroscience 340:530–541.
831 Shippenberg TS, Bals-Kubik R (1995) Involvement of the mesolimbic dopamine system in
832 mediating the aversive effects of opioid antagonists in the rat. Behav Pharmacol 6:99–
833 106.
834 Shippenberg TS, Bals-Kubik R, Huber A, Herz A (1991) Neuroanatomical substrates mediating
835 the aversive effects of D-1 dopamine receptor antagonists. Psychopharmacology (Berl)
836 103:209–14.
837 Sim LJ, Xiao R, Childers SR (1996) Identification of opioid receptor-like (ORL1) peptide-
838 stimulated [35S]GTP gamma S binding in rat brain. Neuroreport 7:729–733.
839 Spampinato S, Di Toro R, Alessandri M, Murari G (2002) Agonist-induced internalization and
840 desensitization of the human nociceptin receptor expressed in CHO cells. Cell Mol Life
841 Sci 59:2172–2183.
842 Spampinato S, Di Toro R, Qasem AR (2001) Nociceptin-induced internalization of the ORL1
843 receptor in human neuroblastoma cells. Neuroreport 12:3159–3163.
844 Spanagel R, Herz A, Shippenberg TS (1992) Opposing tonically active endogenous opioid
845 systems modulate the mesolimbic dopaminergic pathway. Proc Natl Acad Sci U S A
846 89:2046–2050.
847 Spina L, Fenu S, Longoni R, Rivas E, Di Chiara G (2006) Nicotine-conditioned single-trial place
848 preference: selective role of nucleus accumbens shell dopamine D1 receptors in
849 acquisition. Psychopharmacology (Berl) 184:447–55.
850 Thakker DR, Standifer KM (2002) Induction of G protein-coupled receptor kinases 2 and 3
851 contributes to the cross-talk between μ and ORL1 receptors following prolonged agonist
852 exposure. Neuropharmacology 43:979–990.
853 Toledo MA, Pedregal C, Lafuente C, Diaz N, Martinez-Grau MA, Jiménez A, Benito A, Torrado A,
854 Mateos C, Joshi EM, Kahl SD, Rash KS, Mudra DR, Barth VN, Shaw DB, McKinzie D, Witkin
855 JM, Statnick MA (2014) Discovery of a novel series of orally active nociceptin/orphanin

856 FQ (NOP) receptor antagonists based on a dihydrospiro(piperidine-4,7'-thieno[2,3-
857 c]pyran) scaffold. J Med Chem 57:3418–3429.
858 Toll L, Bruchas MR, Calo' G, Cox BM, Zaveri NT (2016) Nociceptin/Orphanin FQ Receptor
859 Structure, Signaling, Ligands, Functions, and Interactions with Opioid Systems.
860 Pharmacol Rev 68:419–457.
861 Tsai H-C, Zhang F, Adamantidis A, Stuber GD, Bonci A, de Lecea L, Deisseroth K (2009) Phasic
862 firing in dopaminergic neurons is sufficient for behavioral conditioning. Science
863 324:1080–1084.
864 Tzschentke TM (2001) Pharmacology and behavioral pharmacology of the mesocortical
865 dopamine system. Progress in Neurobiology 63:241–320.
866 Ungerstedt U (1971) Stereotaxic mapping of the monoamine pathways in the rat brain. Acta
867 Physiol Scand Suppl 367:1–48.
868 Varty GB, Lu SX, Morgan CA, Cohen-Williams ME, Hodgson RA, Smith-Torhan A, Zhang H, Fawzi
869 AB, Graziano MP, Ho GD, Matasi J, Tulshian D, Coffin VL, Carey GJ (2008) The Anxiolytic-
870 Like Effects of the Novel, Orally Active Nociceptin Opioid Receptor Agonist 8-[bis(2-
871 Methylphenyl)methyl]-3-phenyl-8-azabicyclo[3.2.1]octan-3-ol (SCH 221510). J
872 Pharmacol Exp Ther 326:672–682.
873 Vaughan CW, Christie MJ (1996) Increase by the ORL1 receptor (opioid receptor-like1) ligand,
874 nociceptin, of inwardly rectifying K conductance in dorsal raphe nucleus neurones. Br J
875 Pharmacol 117:1609–1611.
876 Vazquez-DeRose J, Stauber G, Khroyan TV, Xie X (Simon), Zaveri NT, Toll L (2013) Retrodialysis
877 of N/OFQ into the nucleus accumbens shell blocks cocaine-induced increases in
878 extracellular dopamine and locomotor activity. Eur J Pharmacol 699:200–206.
879 Vitale G, Arletti R, Ruggieri V, Cifani C, Massi M (2006) Anxiolytic-like effects of
880 nociceptin/orphanin FQ in the elevated plus maze and in the conditioned defensive
881 burying test in rats. Peptides 27:2193–2200.
882 Walker JR, Spina M, Terenius L, Koob GF (1998) Nociceptin fails to affect heroin self-
883 administration in the rat. Neuroreport 9:2243–2247.
884 Wang JB, Johnson PS, Imai Y, Persico AM, Ozenberger BA, Eppler CM, Uhl GR (1994) cDNA
885 Cloning of an orphan opiate receptor gene family member and its splice variant. FEBS
886 Letters 348:75–79.
887 Werling LL, Frattali A, Portoghese PS, Takemori AE, Cox BM (1988) Kappa receptor regulation of
888 dopamine release from striatum and cortex of rats and guinea pigs. J Pharmacol Exp
889 Ther 246:282–286.
890 Winter S, Dieckmann M, Schwabe K (2009) Dopamine in the prefrontal cortex regulates rats
891 behavioral flexibility to changing reward value. Behavioural Brain Research 198:206–
892 213.
893 Wise RA (2005) Forebrain substrates of reward and motivation. J Comp Neurol 493:115–121.

894 Witkin JM, Wallace TL, Martin WJ (2019) Therapeutic Approaches for NOP Receptor Antagonists
895 in Neurobehavioral Disorders: Clinical Studies in Major Depressive Disorder and Alcohol
896 Use Disorder with BTRX-246040 (LY2940094). Handb Exp Pharmacol 254:399–415.
897 Witten IB, Steinberg EE, Lee SY, Davidson TJ, Zalocusky KA, Brodsky M, Yizhar O, Cho SL, Gong S,
898 Ramakrishnan C, Stuber GD, Tye KM, Janak PH, Deisseroth K (2011) Recombinase-driver
899 rat lines: tools, techniques, and optogenetic application to dopamine-mediated
900 reinforcement. Neuron 72:721–733.
901 Xiao C, Shao XM, Olive MF, Griffin 3rd WC, Li KY, Krnjevic K, Zhou C, Ye JH (2008) Ethanol
902 Facilitates Glutamatergic Transmission to Dopamine Neurons in the Ventral Tegmental
903 Area. Neuropsychopharmacology.
904 Zhang NR, Planer W, Siuda ER, Zhao H-C, Stickler L, Chang SD, Baird MA, Cao Y-Q, Bruchas MR
905 (2012) Serine 363 Is Required for Nociceptin/Orphanin FQ Opioid Receptor (NOPR)
906 Desensitization, Internalization, and Arrestin Signaling. J Biol Chem 287:42019–42030.
907 Zheng F, Grandy DK, Johnson SW (2002) Actions of orphanin FQ/nociceptin on rat ventral
908 tegmental area neurons in vitro. Br J Pharmacol 136:1065–1071.
909